CHAPTER 4
SYNTHESIS AND CHARACTERISATION OF COPOLYMERS AND TERPOLYMERS OF L-LACTIDE, ε-CAPROLACTONE AND GLYCOLIDE

In this chapter, the synthesis and characterisation of the various co- and terpolymers of L-lactide, ε-caprolactone and glycolide are described in the sequence:

(1) homopolymer of L-lactide (for reference purposes)
(2) random copolymer of L-lactide and ε-caprolactone (80 : 20)
(3) random terpolymer of L-lactide, ε-caprolactone and glycolide (70 : 20 : 10)
(4) segmented triblock terpolymer of L-lactide, ε-caprolactone and glycolide (70 : 20 : 10)

As mentioned at the end of Chapter 1, one of the main objectives of this project, as seen at its outset, was to compare the fibre properties of random and block terpolymers of similar overall composition. These monofilament fibres were structurally designed for potential use as absorbable surgical sutures. Their target properties were therefore well defined. The synthesis and characterisation methods described here draw heavily on the knowledge and experience gained in previous research projects [55,59] carried out within the Chiang Mai Polymer Research Group.

4.1 Chemicals and Instruments

4.1.1 Chemicals

The chemicals used in this research project were as listed in Table 4.1.

Table 4.1 Chemicals used in this research project.

CHEMICAL	USAGE	GRADE	SUPPLIER
L(+)-lactic acid	Monomer precursor	Purum	Fluka AG
Glycolic acid	Monomer precursor	Puriss	Fluka AG
ε-Caprolactone	Monomer	Lab reagent**	Fluka AG
p-Toluene sulfonic acid	Catalyst	99%	Aldrich
Antimony trioxide	Catalyst	Lab reagent	Fluka AG
Stannous octoate*	Catalyst or initiator	95%	Sigma
Diethylene glycol	Initiator	AR Grade**	Fluka AG
Ethyl acetate	Solvent	Commercial**	Merck
Chloroform	Solvent	Commercial**	Merck
Calcium chloride	Drying agent	Lab reagent	Merck
Calcium hydride	Drying agent	Lab reagent	Merck
Molecular sieves 4 Å	Drying agent	Lab reagent	Merck
Silicone oil	Heating bath	Commercial	Fluka AG

* systematic name = tin(II)-bis-2-ethylhexanoate, ** purified by fractional distillation

4.1.2 Instruments

The main instruments used in this research project were as listed in Table 4.2.

Table 4.2 Instruments used in this research project.

INSTRUMENT	COMPANY	MODEL
FT-IR Spectrometer	Nicolet	510
Differential Scanning Calorimeter	Perkin-Elmer	DSC7
Thermogravimetric Analyzer	Perkin-Elmer	TGA7
75 MHz ^{13}C-NMR Spectrometer	Bruker	DPX-300
300 MHz ^{1}H-NMR Spectrometer	Bruker	DPX-300
Gel Permeation Chromatograph	Waters	150-CV
Automatic Viscosity Measuring System	Schott-Gerate	AVS300
Small-Scale Melt Spinning Apparatus	Bradford University Research Ltd.*	-
Universal Mechanical Testing Machine	Lloyd Instruments	LRX+
Controlled Atmosphere Glove Box	Labconco	50004

* now operating under the name of Ventures Consultancy Bradford (VCB), UK

4.2 Monomer Preparation and Purification

4.2.1 L-lactide and Glycolide

Because the monomers L-lactide and glycolide are prohibitively expensive to buy commercially, they were synthesized from their much cheaper precursors, L(+)-lactic acid and glycolic acid respectively. Each synthesis involved two steps [55]: firstly, the linear polycondensation of the acid to its low molecular weight polymer using p-toluene sulfonic acid (PTSA) as catalyst followed, secondly, by thermal decomposition of the polymer using antimony trioxide as catalyst to yield either L-lactide or glycolide as the primary decomposition product. The apparatus used is shown in Fig. 4.1. The final products were purified at least 4 times by recrystallization from distilled ethyl acetate. The purified L-lactide and glycolide monomers were obtained as white, needle-like and white, leaf-like crystalline solids respectively. They were dried in a vacuum oven at 55°C for 20 hours prior to being transferred into a glove box for use in polymerisation. The chemical equations for the reactions involved in this two-step synthesis are given below for L-lactide.

Step 1

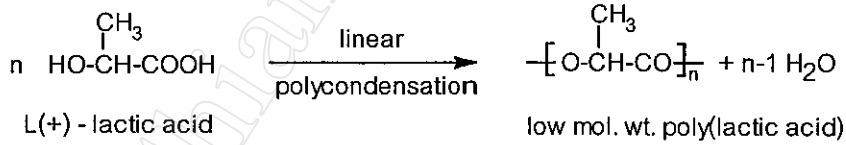

Step 2

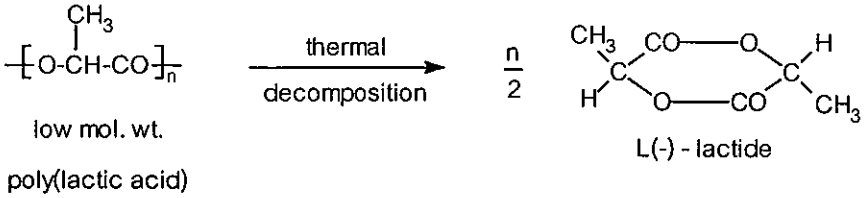

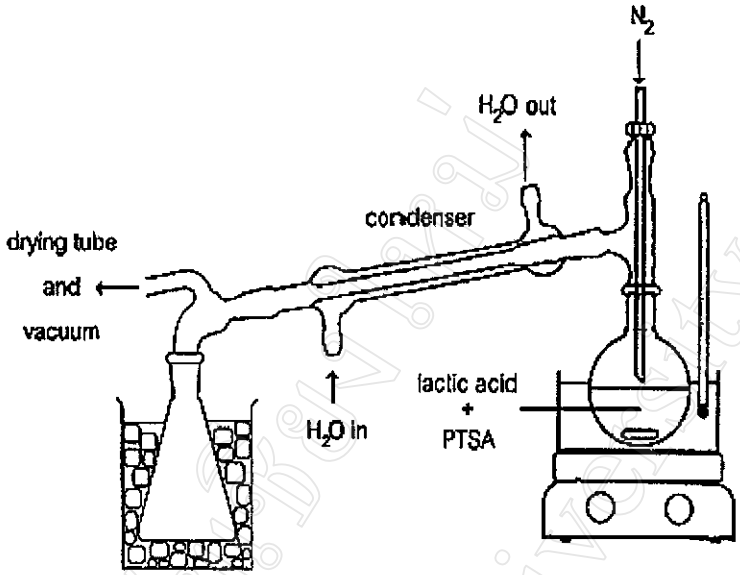

(a)

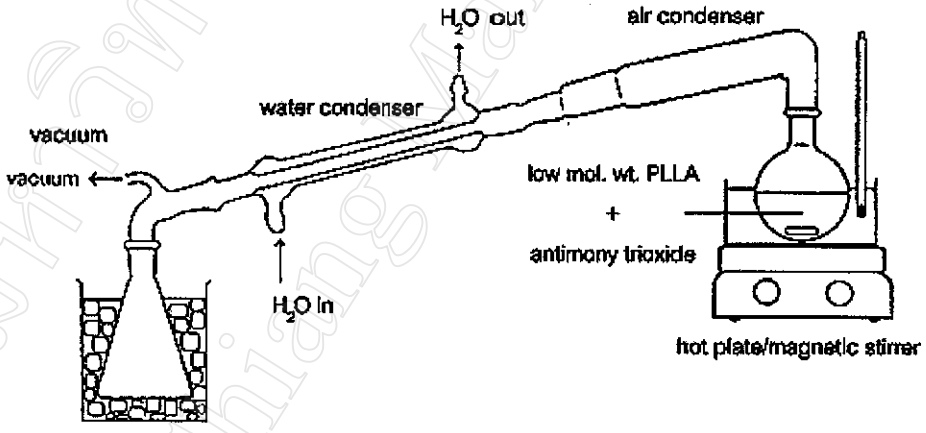

(b)

Fig. 4.1 Apparatus used in the two-step preparation of L-lactide (or glycolide) : (a) L-lactic acid polycondensation to low molecular weight poly(L-lactic acid), PLLA; (b) thermal decomposition of low molecular weight PLLA to L-lactide.

4.2.1.1 Purity Analysis of L-Lactide and Glycolide

Thermal analysis by differential scanning calorimetry (DSC) showed that the purified L-lactide and glycolide each had a sharp melting peak from about 95-97°C and 82-84°C, as shown in Figs. 4.2-4.3 respectively.

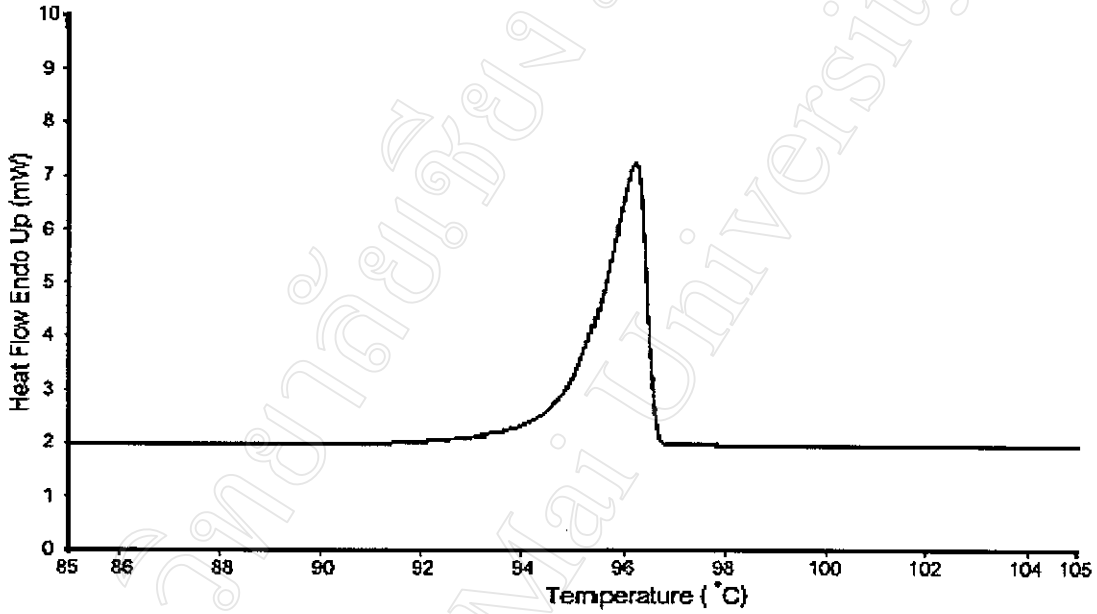

Fig. 4.2 DSC curve of purified L-lactide.

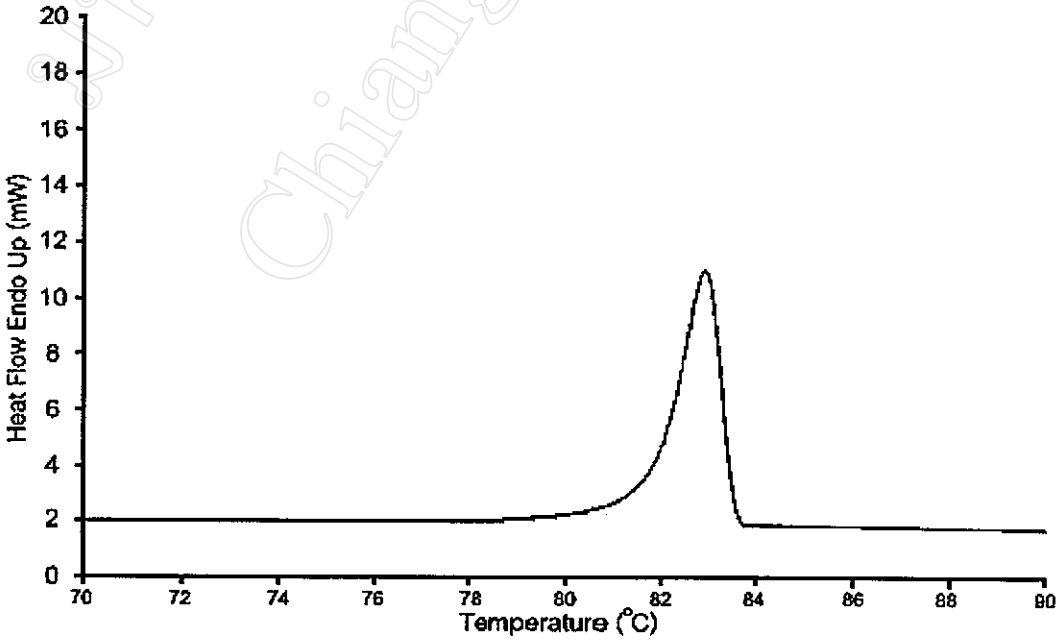

Fig. 4.3 DSC curve of purified glycolide.

In order to determine the actual mole % purities of the purified L-lactide and glycolide from their DSC curves, the instrument's Purity Analysis Software Program was employed. To obtain the best results from purity analysis, a slow scanning rate of 2°C min^{-1} and small sample size in the range of 1-3 mg were used. The DSC7 Purity Analysis Program contains sub-routines that determine a sample's purity by fitting a portion of the melting curve data to a plot of the Van't Hoff Equation, as shown in Figs. 4.4-4.5. As DSC theory predicts, as the impurity content increases, the melting point decreases and the melting range broadens. From their respective DSC curves and Van't Hoff plots, chemical purities of 99.92% and 99.83% (by mole) were obtained for the purified L-lactide and glycolide monomers. These purities were considered to be sufficiently high (>99.5%) for the monomers to be able to yield sufficiently high molecular weight polymers for fibre spinning.

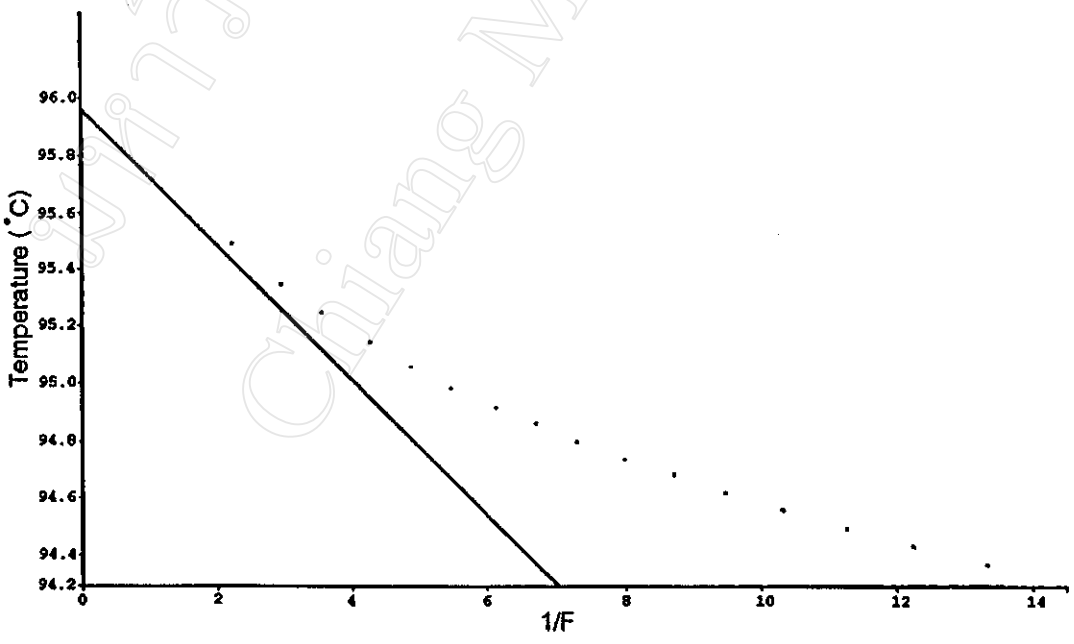

Fig. 4.4 Van't Hoff plot of the purity analysis data for the purified L-lactide.
(F = mole fraction of the sample which has melted)

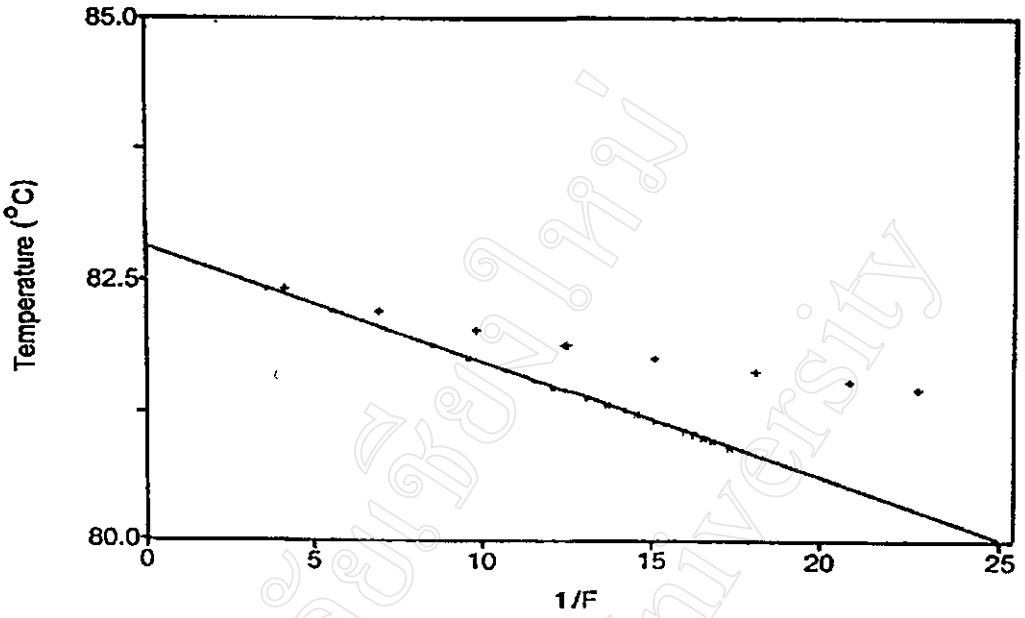

Fig. 4.5 Van't Hoff plot of the purity analysis data for the purified glycolide.
(F = mole fraction of the sample which has melted)

4.2.2 ε-Caprolactone

Commercial ε-caprolactone was purified by drying over CaH_2 for 48 hours before being vacuum distilled. During its vacuum distillation, the constant boiling fraction at 75°C/2 mm Hg (cf., lit. [56] b. pt. = 82°C/5.5 mm Hg) was collected. Pure ε-caprolactone was obtained as a clear colourless liquid at room temperature. It was stored over molecular sieves (4 Å) in a refrigerator in a tightly sealed container until required for use in polymerisation.

4.3 Homo-, Co-, and Terpolymer Syntheses

4.3.1 Poly(L-lactide) Homopolymer

Since L-lactide was to be the major component (≈ 70% by mole) in the terpolymers, it was considered useful to include poly(L-lactide) homopolymer in the synthesis series so that it could be viewed as a reference polymer against which the terpolymers could be compared. In this way, the effects on fibre properties of incorporating the 2 modifying monomers, ε-caprolactone and glycolide, in the poly (L-lactide) chain could be more easily observed.

Poly(L-lactide) homopolymer was synthesized by the ring-opening polymerization of L-lactide in bulk using $Sn(Oct)_2$ as initiator. All glassware and a magnetic stirrer bar were dried at 150°C overnight and allowed to cool in a dry high-purity nitrogen atmosphere in a glove box before use. A 50 ml round-bottomed flask was charged with the L-lactide monomer and 0.01 mol % of $Sn(Oct)_2$ in the glove box at room temperature. The flask was then closed with a glass stopper, removed from the glove box and immediately immersed in a silicone oil bath at 140°C for 72 hours. At the end of this period, the flask was allowed to cool to room temperature. The final poly(L-lactide) product was removed from the flask and ground up before being dried to constant weight at 100°C in a vacuum oven for 48 hours.

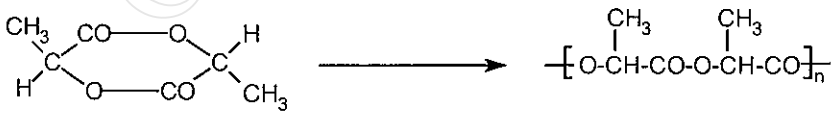

L(-) - lactide poly(L-lactide)

4.3.2 Poly(L-lactide-co-ε-caprolactone) Random Copolymer

A random copolymer of L-lactide and ε-caprolactone (80 : 20 mole % ratio) was synthesized in bulk employing a similar procedure to that just described for L-lactide alone. 0.32 moles of L-lactide, 0.08 moles of ε-caprolactone and 0.0004 moles (0.1 mole %) of $Sn(Oct)_2$ were weighed into a 100 ml round-bottomed flask equipped with a magnetic stirrer bar in a glove box. The flask was then immersed in a silicone oil bath at 140°C for 72hrs. After cooling to room temperature, the P(LC) copolymer product was cut up into small pieces and dried to constant weight in a vacuum oven at 100°C for 24 hrs.

This P(LC) 80 : 20 composition has been studied in earlier research projects [57, 58] in the Chiang Mai Polymer Research Group and has been shown to have good fibre-forming properties. It therefore seemed to be a logical starting point for this work prior to modifying both the composition and microstructure.

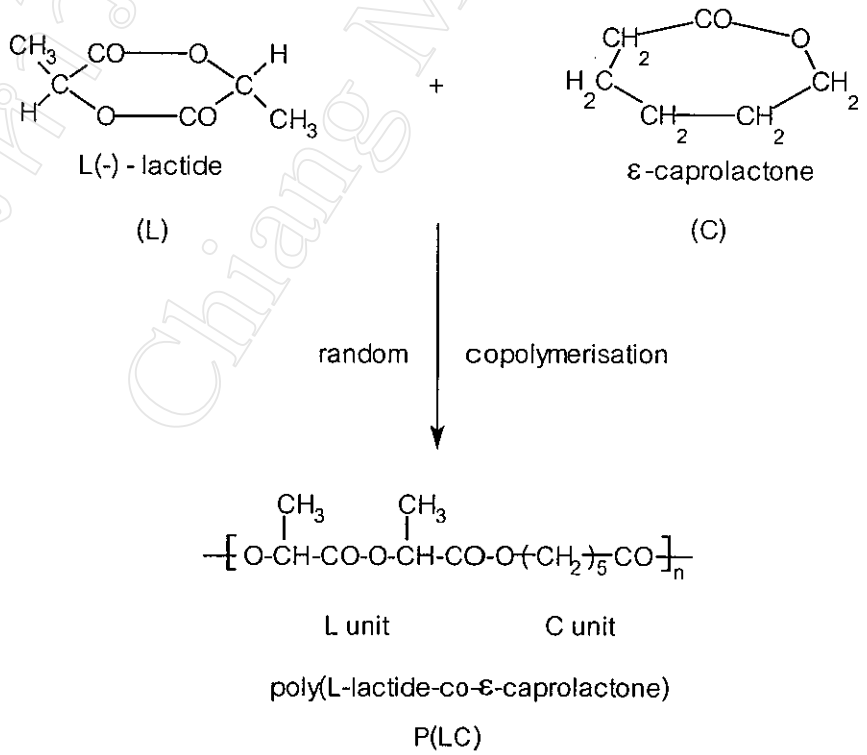

4.3.3 Poly(L-lactide-co-ε-caprolactone-co-glycolide) Random Terpolymers

Since the emphasis in this research project was on fibre processing and property testing rather than polymer synthesis, the terpolymer composition to be studied (70 : 20 : 10) and the synthesis conditions to be employed were decided upon from the results of previous work [57,59] within the Chiang Mai Polymer Research Group. These conditions have already been extensively studied and have been shown to produce molecular weights which should be high enough ($\bar{M}_n$ > 50,000) for melt spinning.

The ring-opening random terpolymerisations of L-lactide, ε-caprolactone and glycolide, each using a monomer mole ratio of 70:20:10, were conducted in bulk using the different catalyst / initiator combinations shown in Table 4.3. Each terpolymerisation was conducted in the same manner as for the homopolymerisation of poly(L-lactide), employing a polymerisation temperature and time of 140°C and 72 hours respectively. Finally, the crude P(LCG) terpolymers were cut into small pieces before being dried in a vacuum oven at 90°C for 48 hours to constant weight to ensure removal of any residual monomers.

Table 4.3 Conditions used in the random terpolymerisations of L-lactide, ε-caprolactone and glycolide.

Terpolymer Code*	$Sn(Oct)_2$ (mol %)	DEG** (mol %)	$Sn(Oct)_2$/DEG Mode of Addition***
P(LCG) 1	0.02	-	-
P(LCG) 2	0.02	0.04	Pre-mixed
P(LCG) 3	0.02	0.04	Separate

* P(LCG) = poly(L-lactide-*co*-ε-caprolactone-*co*-glycolide)
= P(LL-*co*-CL-*co*-G)

** DEG = diethylene glycol (initiator)

*** $Sn(Oct)_2$/DEG either pre-mixed or added separately

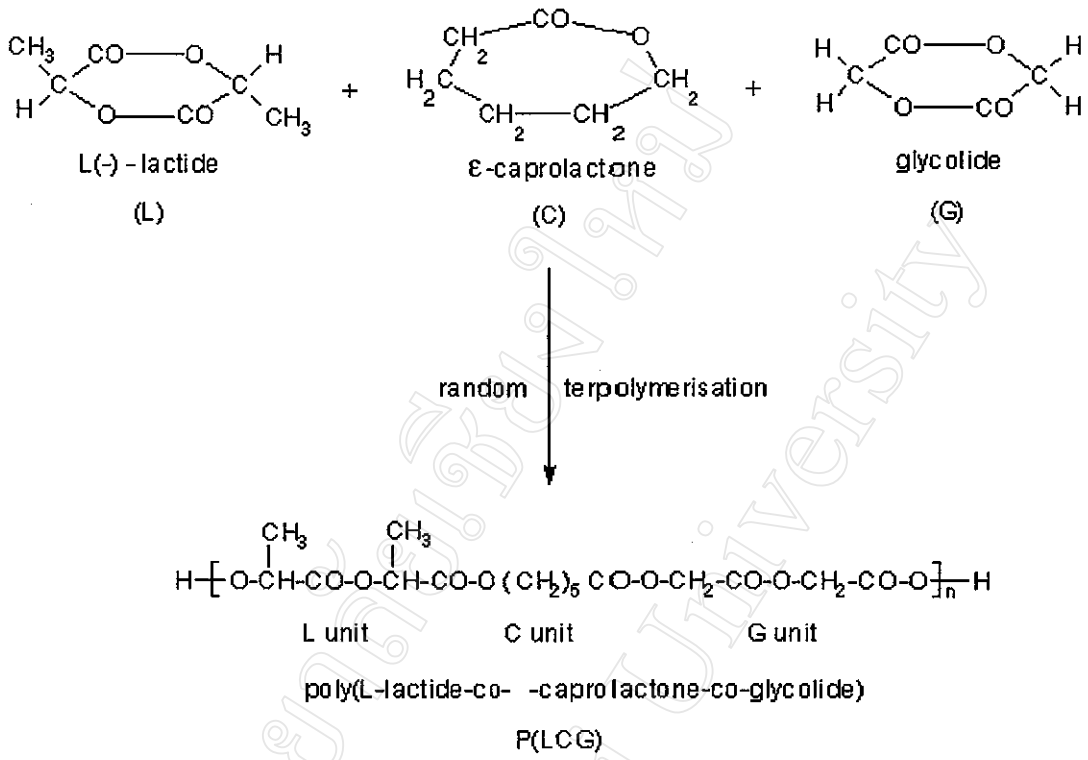

4.3.4 Poly(L-lactide-co-ε-caprolactone-co-glycolide) Triblock Terpolymer

One of the main interests in this work was to see how terpolymers of similar composition but different microstructures compared with respect to their melt spinning and fibre properties. Thus, a segmented triblock P(LCG) terpolymer of similar 70 : 20 : 10 mol % composition to the random P(LCG) terpolymers was designed and synthesized as follows.

A segmented triblock terpolymer (A-B-A) composed of side blocks (A) of a random copolymer of L-lactide and glycolide and a centre block (B) of a random copolymer of L-lactide and ε-caprolactone was synthesized via a two-step polymerisation using $Sn(Oct)_2$ and DEG as catalyst and initiator respectively. In the first step, a 100 ml round-bottomed flask with a magnetic stirrer bar was charged with 0.52 mole of L-lactide, 0.52 mole of ε-caprolactone, 0.34 ml of DEG and 0.06 ml of a 0.86 M $Sn(Oct)_2$ solution in dry toluene under a high-purity nitrogen atmosphere in a glove box.

The flask was closed with a glass stopper, removed from the glove box and immediately immersed in a silicone oil bath at 140°C for 12 hours (see Scheme 4.1 (a)). At the end of the polymerisation period, the flask was allowed to cool to room temperature, the P(LC) copolymer removed from flask and cut into small pieces (2-3 mm). Finally, it was dried at 55°C in a vacuum oven for 20 hours prior to its structural characterisation.

In the second step, two end blocks of a random copolymer of L-lactide and glycolide were added onto the two OH-terminated chain ends of the P(LC) prepolymer from the first step (see Scheme 4.1 (b)). In this second step, 25.83 g of the P(LC) prepolymer, 0.25 mole of L-lactide, and 0.05 mole glycolide were weighed into a 100 ml round-bottomed flask with a magnetic stirring bar in a glove box. The flask was closed with a glass stopper, removed from the glove box, and immediately immersed in a silicone oil bath at 170°C with vigorous magnetic stirring for 20 min to ensure homogeneous mixing. The oil bath temperature was then decreased to 150°C with slower stirring for 10 hours. The final polymer product was removed from the flask and cut into small pieces (2-3 mm) before being dried in a vacuum oven at 100°C for 10 hours to remove any unreacted monomers.

It should be mentioned here that, when $Sn(Oct)_2$ is used in conjunction with DEG, the DEG takes over the role of initiator in the coordination-insertion mechanism, while the $Sn(Oct)_2$ assumes the role of catalyst. Thus, the OH-terminated P(LC) prepolymer from the first step acts as the macroinitiator in the second step leading to the formation of the triblock terpolymer with the macroinitiator as the centre block.

(a) First step :

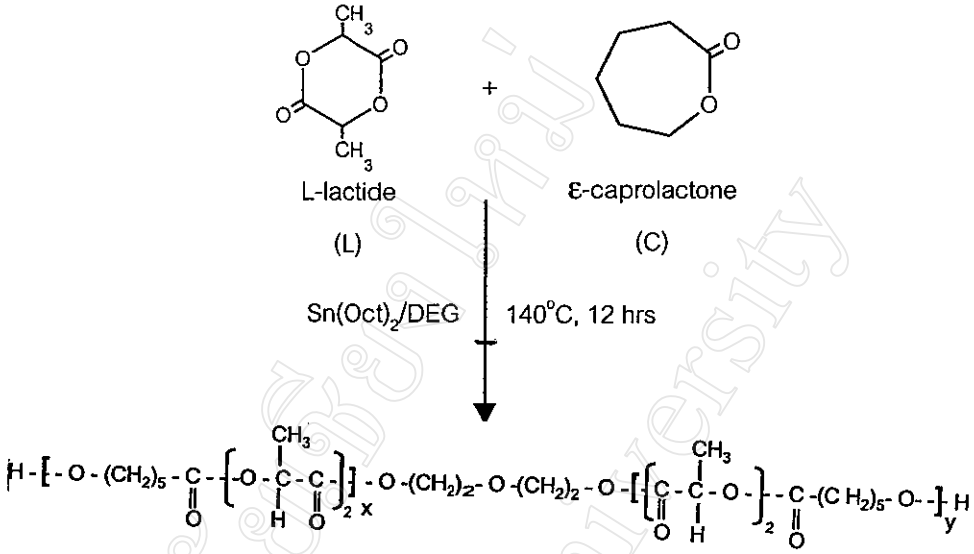

P(LC) prepolymer (50:50)

(b) Second step:

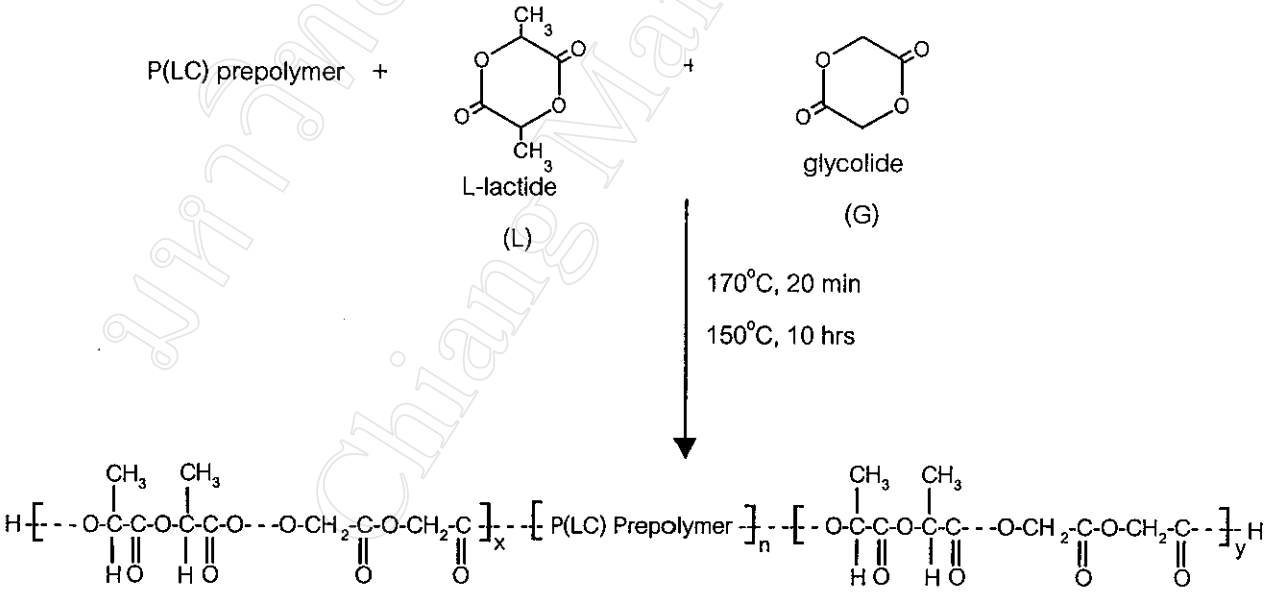

P(LCG) Triblock Terpolymer (70 : 20 : 10)

Scheme 4.1 : Two-step preparation of the P(LCG) triblock terpolymer

(a) First step, P(LC) prepolymer synthesis

(b) Second step, P(LCG) triblock terpolymer synthesis

4.4 Polymer Characterisation

The final polymer products were characterised by a combination of analytical techniques with respect to their chemical structure by FT-IR, chemical composition by ^{1}H-NMR, chain microstructure by ^{13}C-NMR, temperature transitions by DSC, thermal stability by TG, and molecular weight by GPC and dilute-solution viscometry. The results from all of these techniques are now described.

4.4.1 Fourier - Transform Infrared Spectroscopy

The Fourier-transform infrared (FT-IR) spectra of the polymer products are shown in Figs. 4.9-4.13 and can be compared with the homopolymer reference spectra in Figs. 4.6-4.8. All of the product spectra were obtained from samples prepared in the form of thin films cast from solution in chloroform on a NaCl cell. The major peak assignments are as listed in Table 4.4.

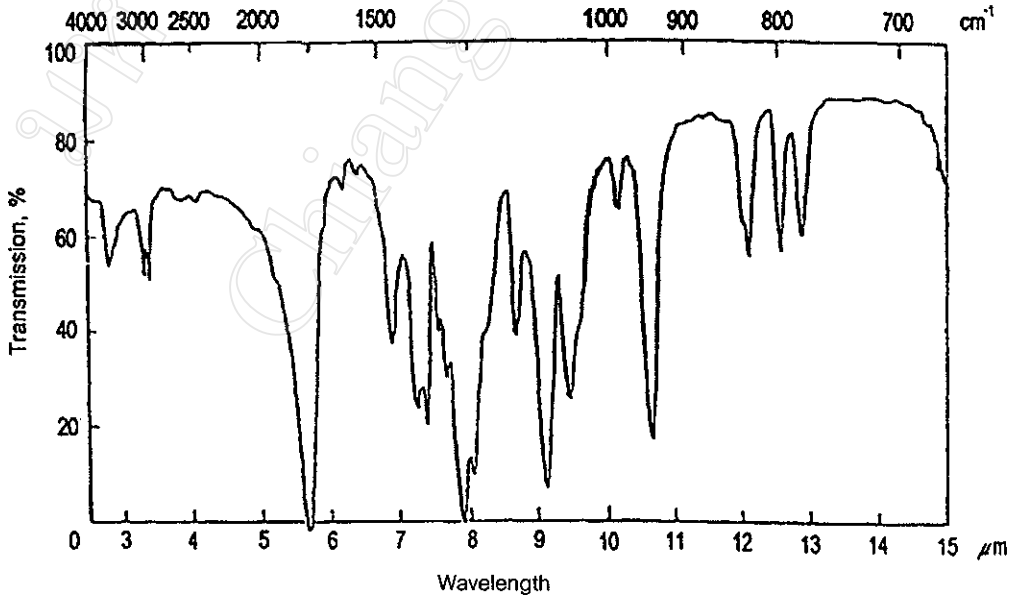

Fig. 4.6 Reference infrared spectrum of poly(L-lactide), PL [60].

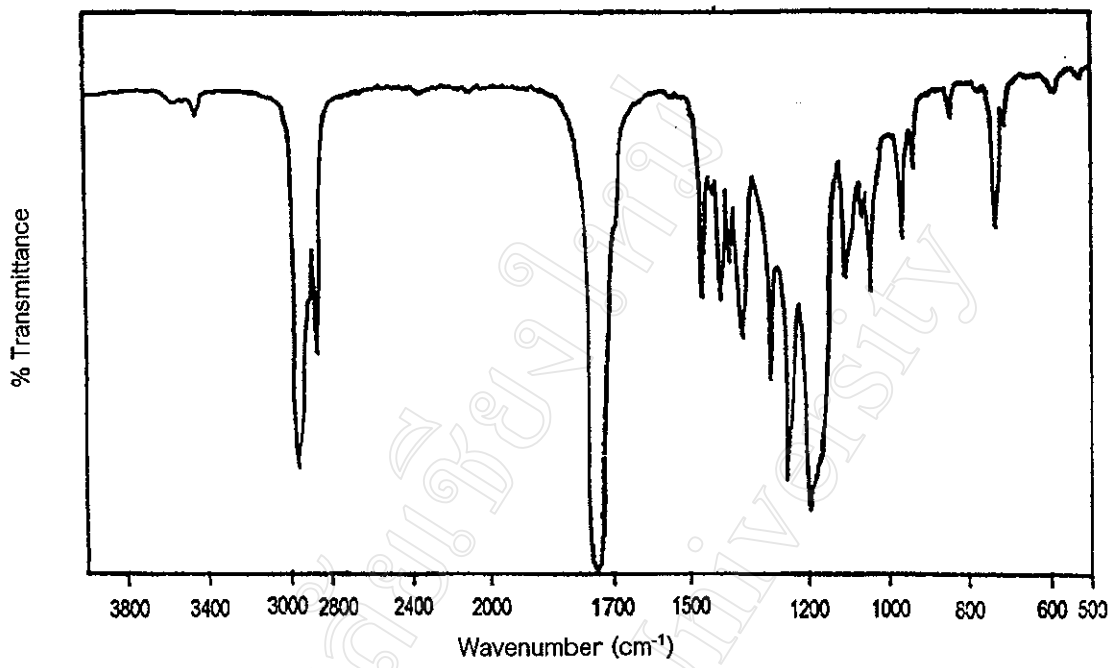

Fig. 4.7 Reference infrared spectrum of poly(ε-caprolactone), PCL [61].

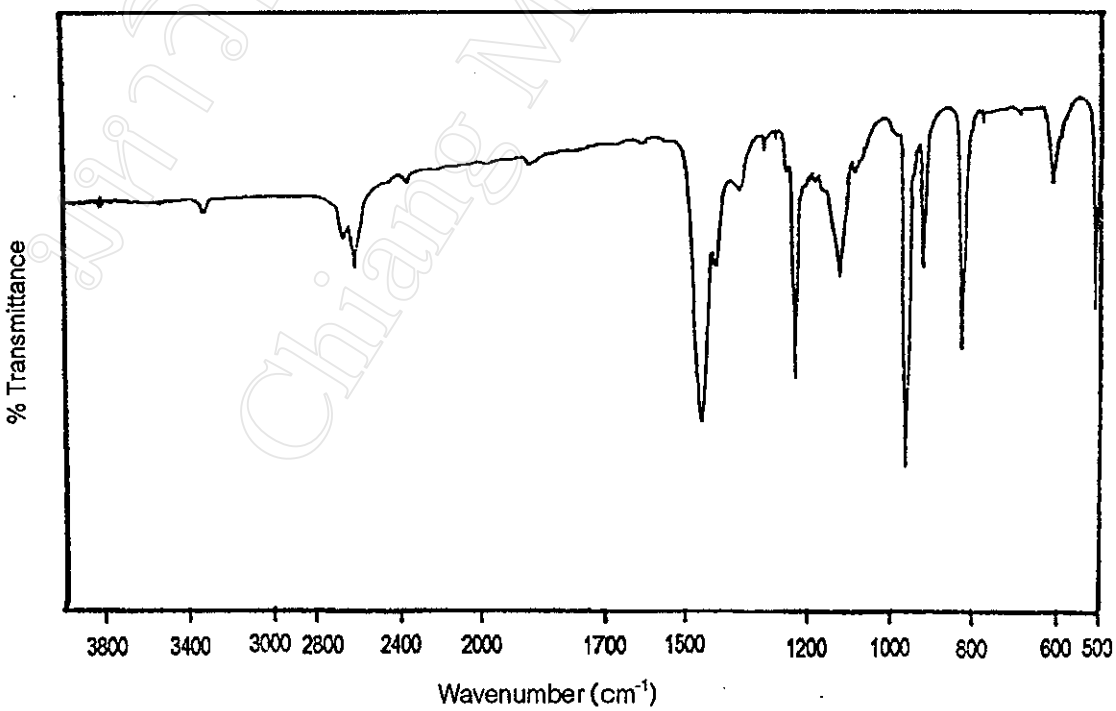

Fig. 4.8 Reference infrared spectrum of polyglycolide, PG [62].

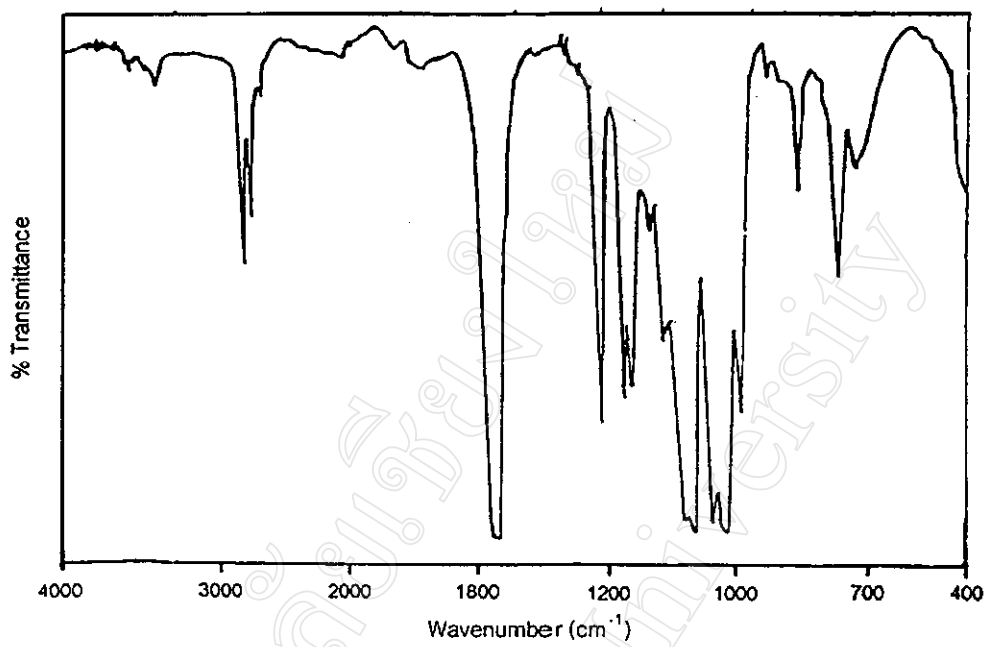

Fig. 4.9 FT-IR spectrum of the synthesized poly(L-lactide), PL.

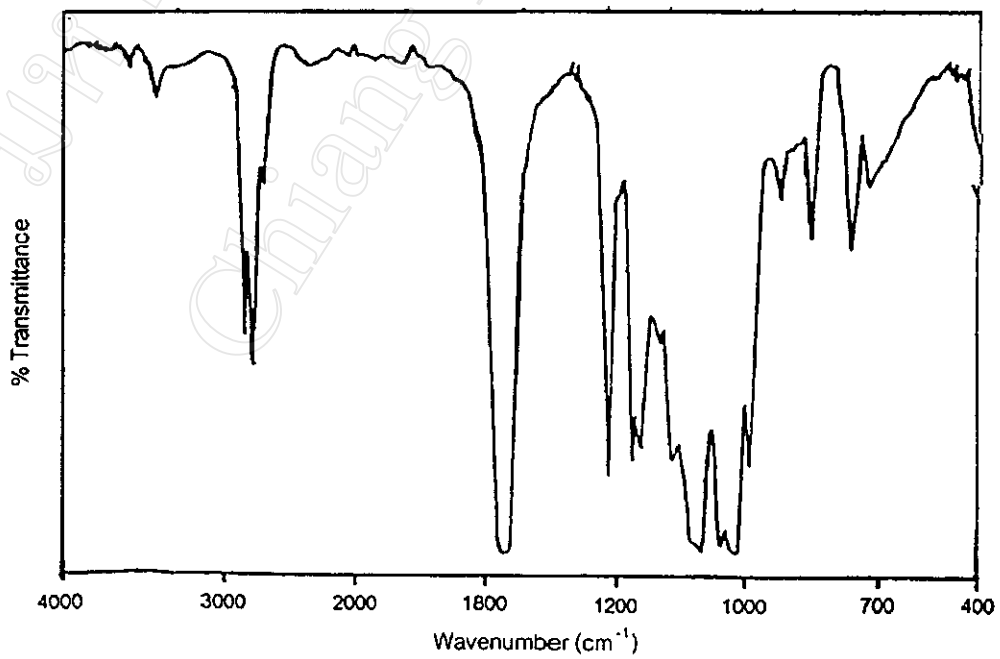

Fig. 4.10 FT-IR spectrum of the P(LC) 80:20 random copolymer.

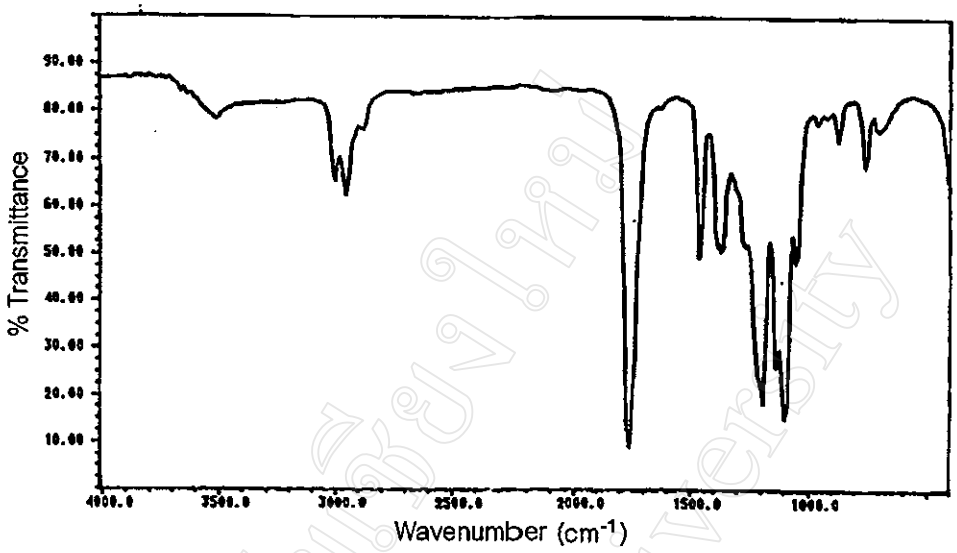

Fig. 4.11 FT-IR spectrum of the P(LCG) 1 70:20:10 random terpolymer.

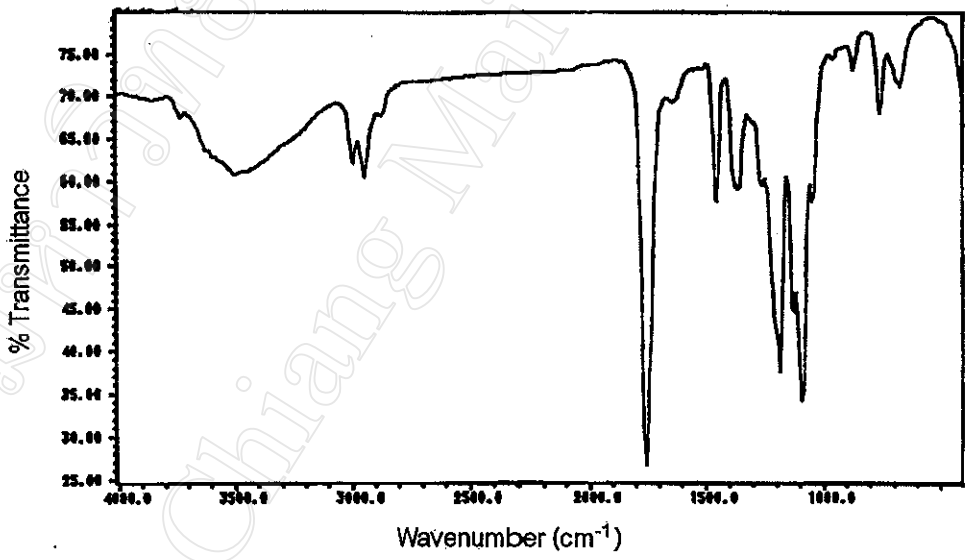

Fig. 4.12 FT-IR spectrum of the hydroxyl-terminated P(LC) 50:50 prepolymer.

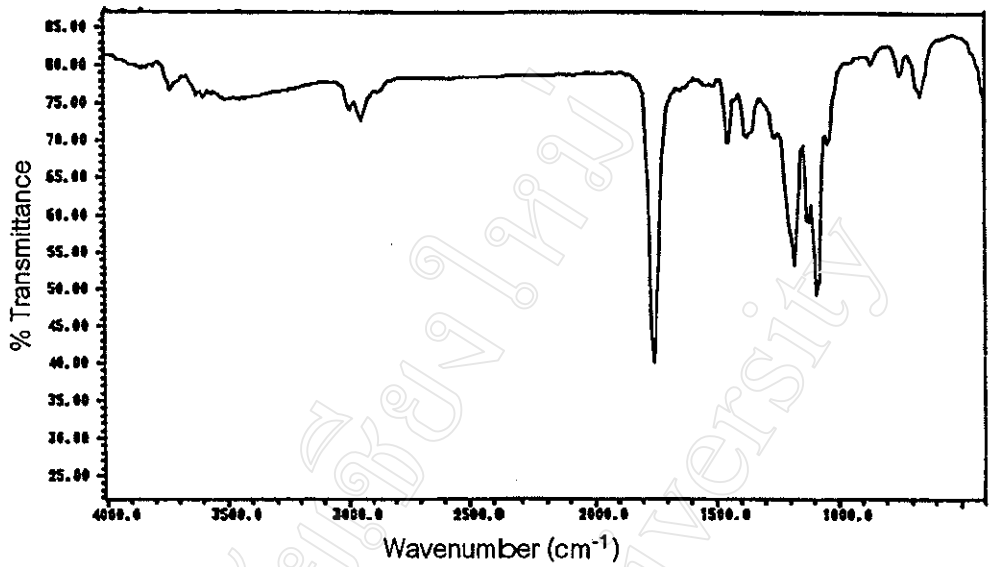

Fig. 4.13 FT-IR spectrum of the P(LCG) 70:20:10 triblock terpolymer.

The IR spectra of the terpolymer products are so similar as to render it impossible to detect their compositional and microstructural differences.

One of the most obvious differences is in the size of the broad O-H stretching band centred at around 3500 cm^{-1} which comes from the OH end-groups. This is particularly noticeable when comparing the P(LC) prepolymer and P(LCG) triblock spectra in Figs. 4.12 and 4.13. As the molecular weight increases in going from the prepolymer to the triblock, the OH chain-end concentration decreases leading to a corresponding decrease in the O-H band. As L-lactide is by far the major component, the terpolymer spectra not surprisingly resemble that of the poly(L-lactide) (PL) homopolymer. Also, the PL, poly(ε-caprolactone) (PCL) and polyglycolide (PG) homopolymer spectra are themselves very similar in appearance, as would be expected from the homopolymers' similar chemical structures.

Table 4.4 Peak assignments and vibrational frequencies in the homo-, co- and terpolymer IR spectra.

Wavenumber (cm^{-1})							Vibrational Assignment
PL (Ref.)	PCL (Ref.)	PG (Ref.)	PLL* Homo	P(LCG) 1 Random	P(LC) Copolymers	P(LCG) Triblock	
3400-3600	3400-3600	3400-3600	3400-3600	3400-3600	3200-3900	-	O-H stretching in alcohol (chain ends)
2950-3000	2850-2950	2950-3000	2900-3000	2850-3000	2850-3000	2850-3000	C-H stretching in CH, CH_2, CH_3
1750	1723	1750	1750	1755	1750	1750	C=O stretching
1450	1450	1450	1450	1460	1460	1460	C-H bending in CH, CH_2, CH_3
1280	1280-1300	1280-1300	1280	1280-1300	1285-1300	1285-1300	C-O stretching in acyl-oxygen
1090	1060	1082	1090	1100	1100	1100	C-O stretching in alkyl-oxygen
-	720	-	-	715	710	710	CH_2 bending (rocking)

* as synthesized in this research project

4.4.2 Nuclear Magnetic Resonance Spectroscopy (^{1}H-NMR and ^{13}C-NMR)

4.4.2.1 Proton Nuclear Magnetic Resonance Spectroscopy (^{1}H-NMR)

The 60 MHz ^{1}H-NMR spectra of the homo-, co-, and terpolymer products in deuterated chloroform ($CDCl_3$) solutions were recorded with tetramethylsilane (TMS) as internal standard at room temperature. The spectra are shown in Figs. 4.14-4.20 including the peak area integrations from which the respective co- and terpolymer compositions could be determined. From the ^{1}H-NMR spectra, resonances specific to each of the 3 different monomer units can be readily identified at δ = 5.0-5.3 ppm (methine C-H in the L units), δ = 2.2-2.5 and 4.0-4.2 ppm (α-CH_2 and ε-CH_2 respectively in the C units) and δ = 4.5-4.9 ppm (CH_2 in the G units). From the peak area integrations of the peaks b, c and h in Figs. 4.15-4.20, the co- and terpolymer chemical compositions are calculated and the results compared with the initial co- and termonomer feeds, as shown in Table 4.5. A sample calculation is given below.

<u>Compositional Analysis of the P(LCG)1 Terpolymer</u>

From the NMR spectrum of the PLCG)1 terpolymer in Fig. 4.16 and the peak area integrations for protons b, c and h, the terpolymer composition is calculated as follows:

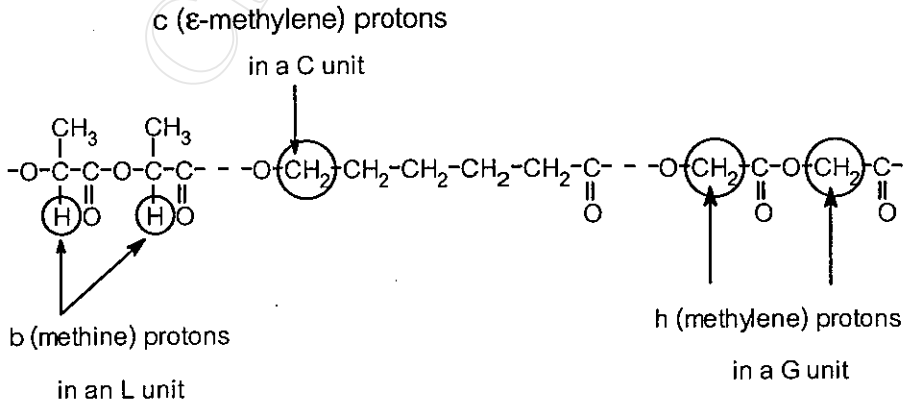

peak integration of methine protons (2H/L unit)		peak integration of ε-methylene protons (2H/C unit)		peak integration of methylene protons (4H/G unit)
$\frac{0.222}{2}$	:	$\frac{0.069}{2}$	:	$\frac{0.062}{4}$
0.111	:	0.0345	:	0.0155

Thus, the terpolymer composition is:

L : C : G	=	0.111	: 0.0345	:	0.0155	
	=	68.94	: 21.42	:	9.63	mol %
	≅	69	: 21	:	10	mol %

This L : C : G terpolymer composition of 70 : 19 : 11 compares very closely with the initial termonomer feed ratio of 70 : 20 : 10. The other co- and terpolymer compositions are calculated similarly from their NMR spectra and the results compared in Table 4.5.

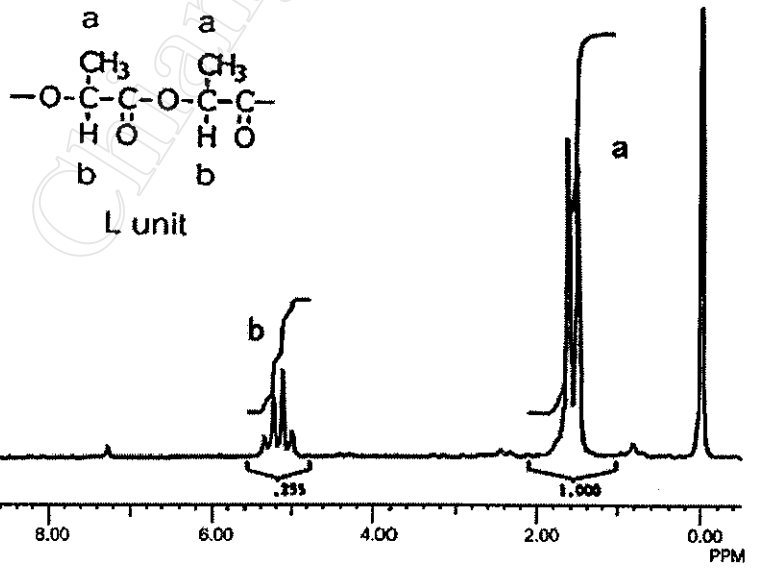

Fig. 4.14 60 MHz ^{1}H-NMR spectrum of the PL homopolymer.

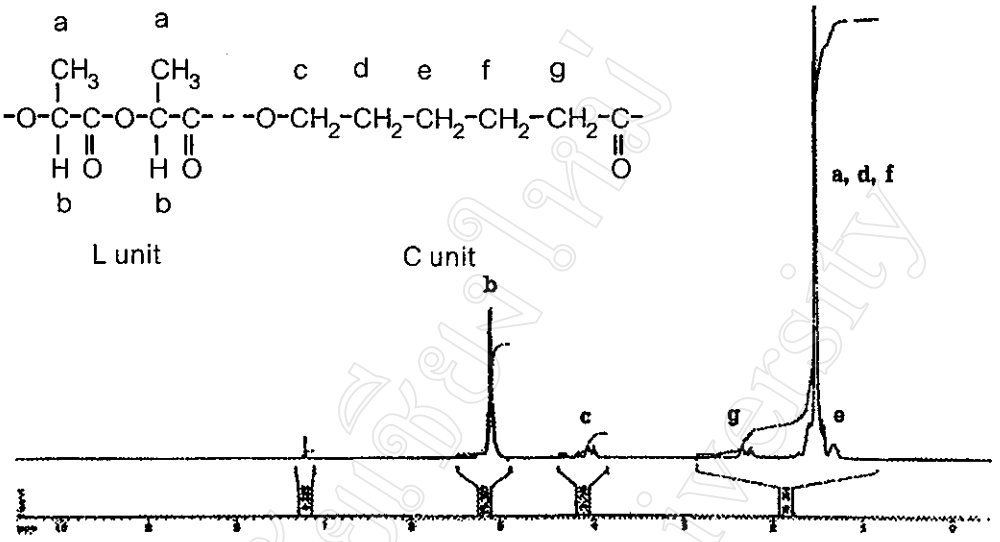

Fig. 4.15 300 MHz ^{1}H-NMR spectrum of the P(LC) 80:20 random copolymer.

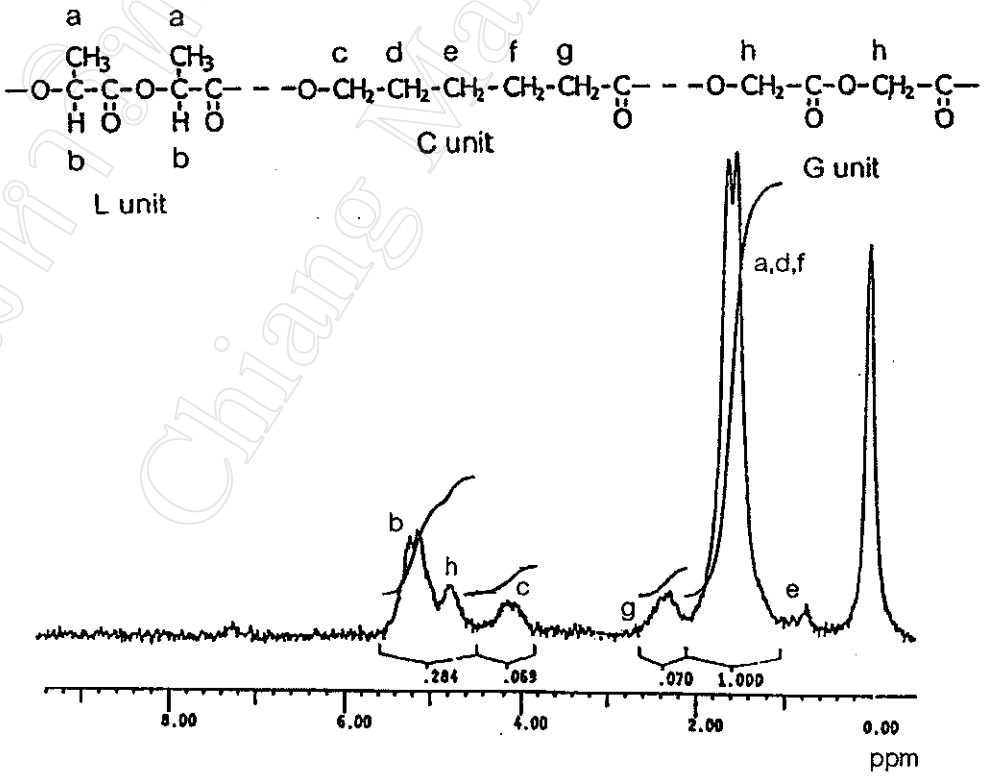

Fig. 4.16 60 MHz ^{1}H-NMR spectrum of the P(LCG) 1 70 : 20 : 10 random terpolymer.

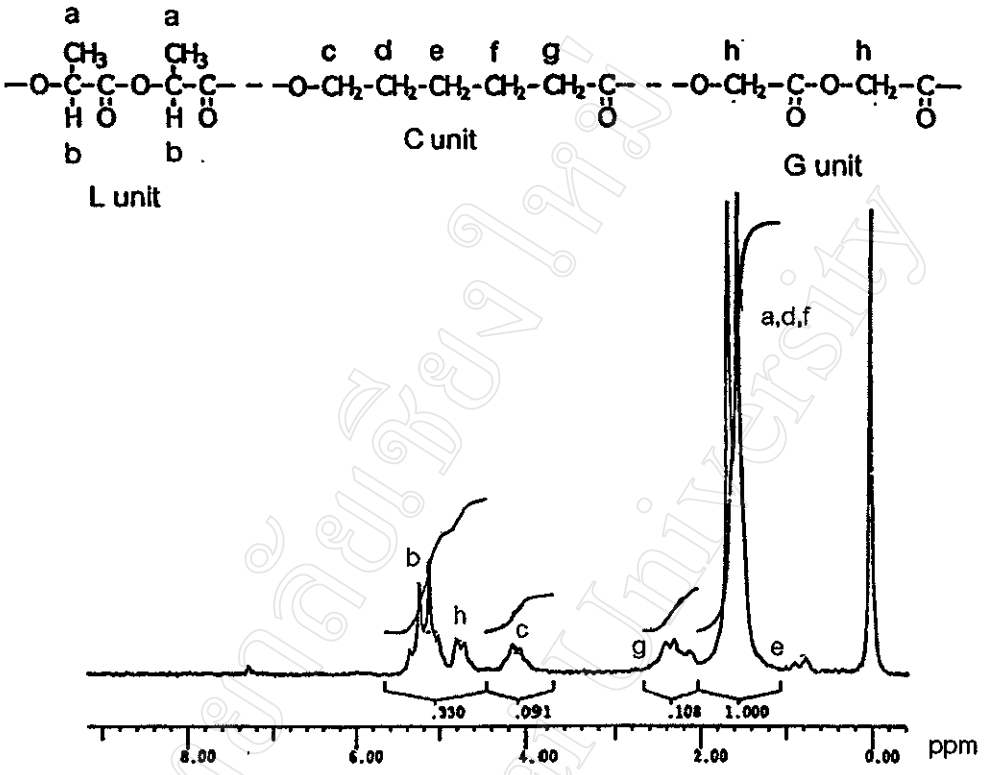

Fig. 4.17 60 MHz ^{1}H-NMR spectrum of the P(LCG) 2 70 : 20 : 10 random terpolymer.

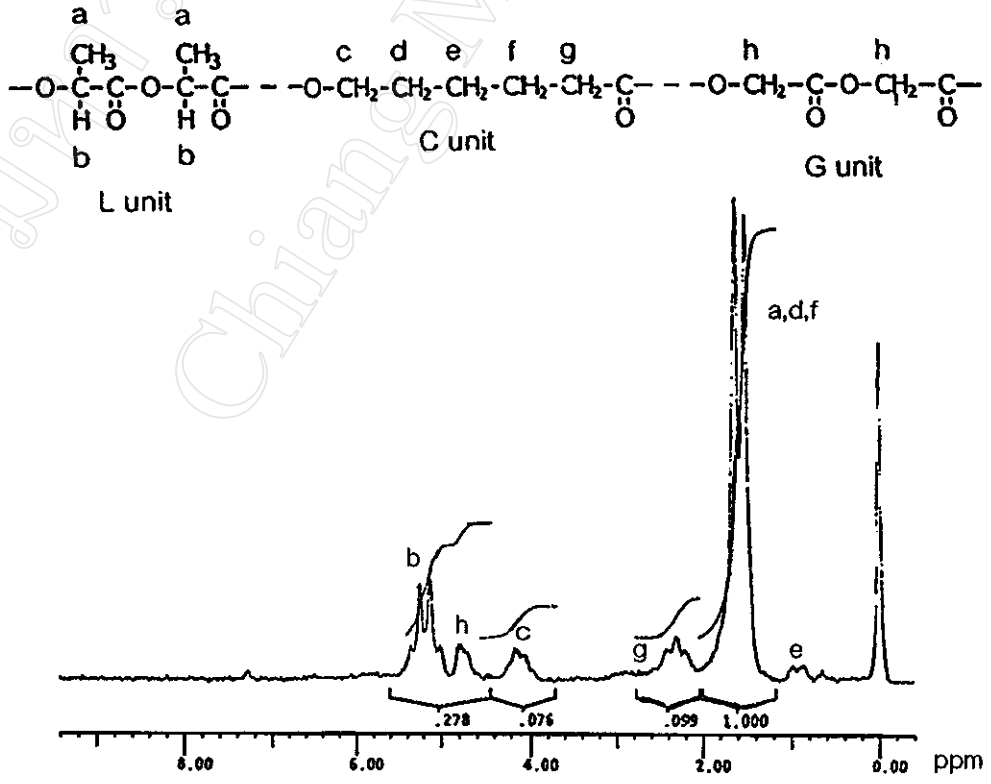

Fig. 4.18 60 MHz ^{1}H-NMR spectrum of the P(LCG) 3 70 : 20 : 10 random terpolymer.

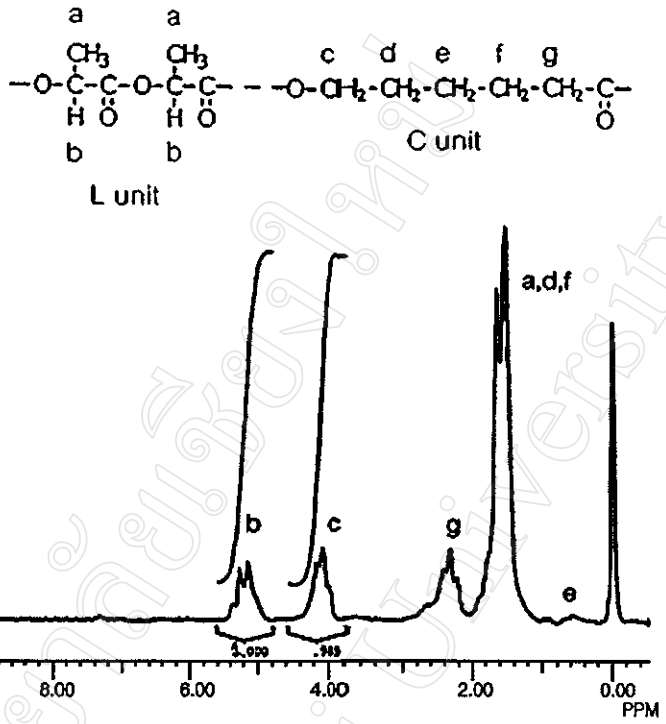

Fig. 4.19 60 MHz ^{1}H-NMR spectrum of the hydroxyl-terminated P(LC) 50 : 50 prepolymer.

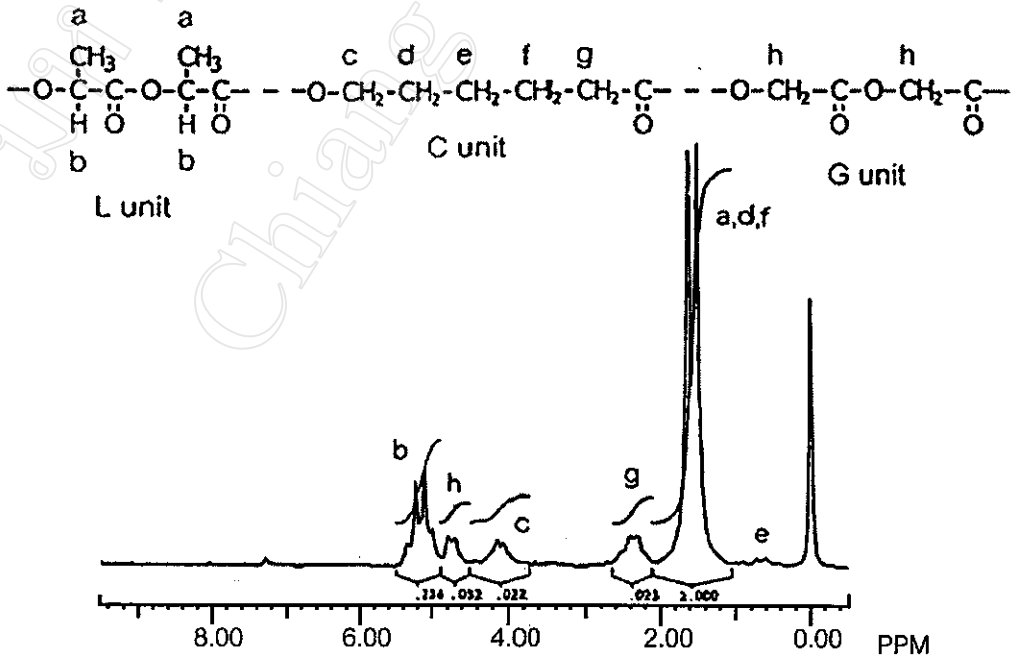

Fig. 4.20 60 MHz ^{1}H-NMR spectrum of the P(LCG) 70 : 20 : 10 triblock terpolymer.

The results in Table 4.5 clearly show that the initial monomer feeds and the final polymer compositions are very similar. These results are consistent with the synthesis reactions having been taken to near completion so that almost all of the initial monomers went into forming the final polymer. What little residual monomer did remain could be estimated from the weight loss (generally < 5%) that occurred on vacuum drying to constant weight.

Table 4.5 Comparison of the initial co- and termonomer feeds with the final co- and terpolymer compositions.

Polymer Products	Initial Monomer Feed L:C:G (mol %)	Final Polymer Composition L:C:G (mol %)
P(LC) Copolymer	80 : 20 : 0	79 : 21 : 0
P(LCG) 1	70 : 20 : 10	69 : 21 : 10
P(LCG) 2	70 : 20 : 10	69 : 22 : 9
P(LCG) 3	70 : 20 : 10	69 : 23 : 8
P(LC) Prepolymer	50 : 50 : 0	50 : 50 : 0
P(LCG) Triblock	70 : 20 : 10	66 : 20 : 14

4.4.2.2 Carbon-13 Nuclear Magnetic Resonance Spectroscopy (^{13}C-NMR)

The main purpose of this ^{13}C-NMR study was to try to obtain microstructural information about the co- and terpolymers that ^{1}H-NMR was unable to provide. This is made possible by the fact that, in ^{13}C-NMR, the chemical shifts are spread over a wide range of over 200 ppm, as compared with the relatively narrow 10 ppm range in ^{1}H-NMR. Therefore, much smaller differences in chemical environment can be distinguished in ^{13}C-NMR making it a much more powerful techinique than ^{1}H-NMR for studying polymer microstructure, in particular monomer sequencing in co- and terpolymers.

In this research project, 75 MHz ^{13}C-NMR spectra of the homo-, co- and terpolymers were obtained using a Bruker Advance DPX-300 Nuclear Magnetic Resonance Spectrometer. The samples were run in deuterated chloroform solutions at room temperature giving the spectra as shown in Figs. 4.21-4.25.

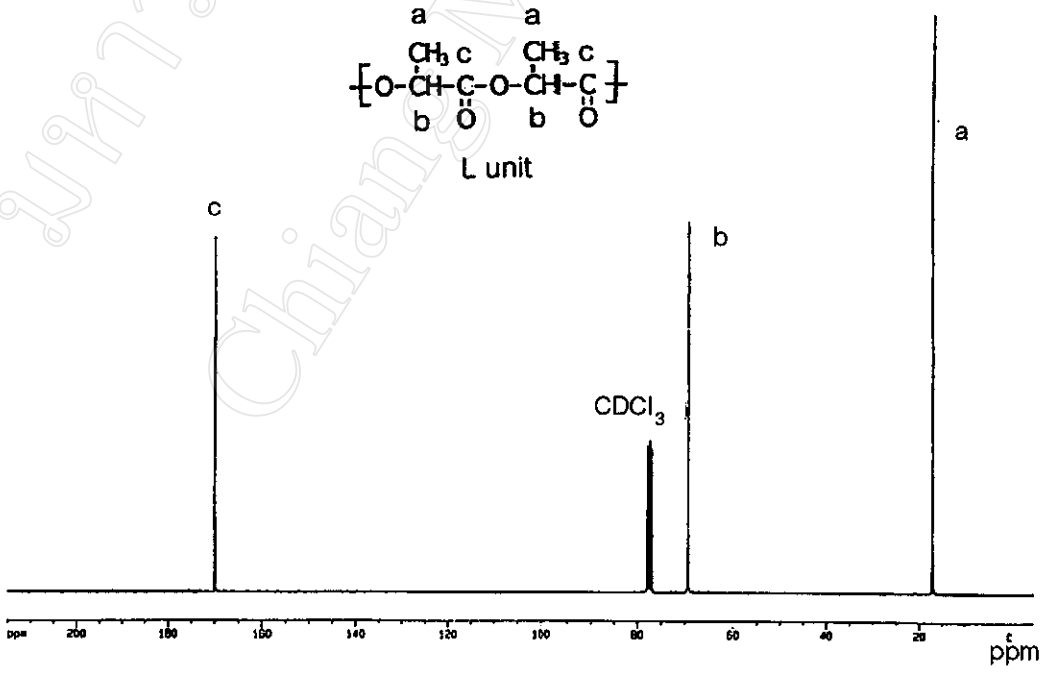

Fig. 4.21 75 MHz ^{13}C-NMR spectrum of the PL homopolymer.

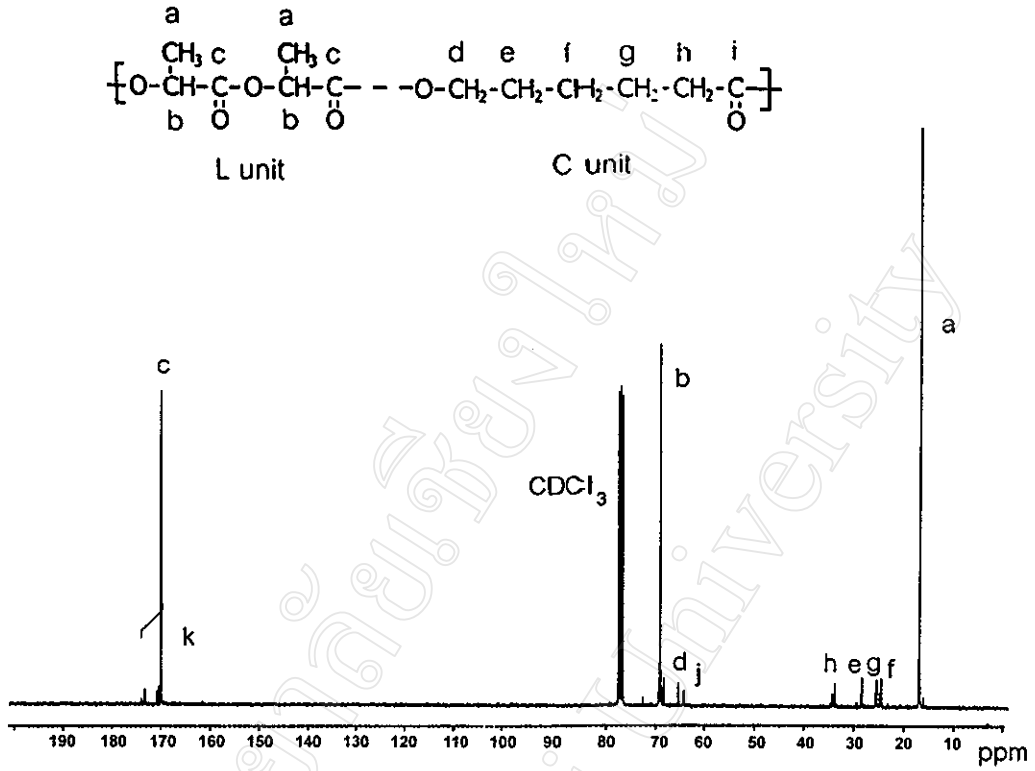

Fig. 4.22 75 MHz ^{13}C-NMR spectrum of the P(LC) 80 : 20 random copolymer.

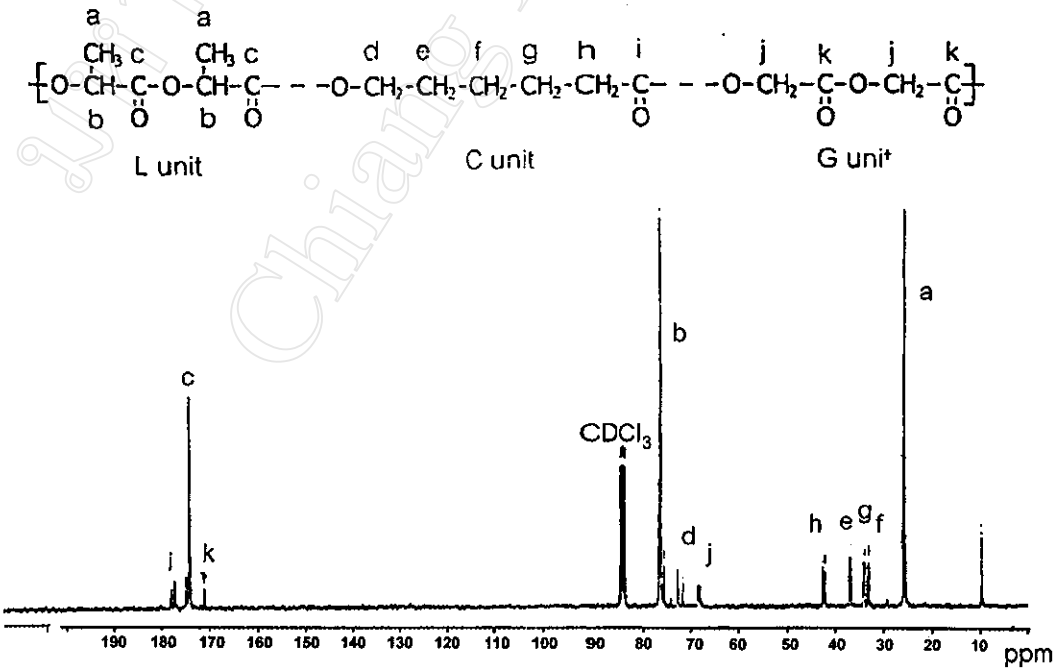

Fig. 4.23 75 MHz ^{13}C-NMR spectrum of the P(LCG) 1 70 : 20 : 10 random terpolymer.

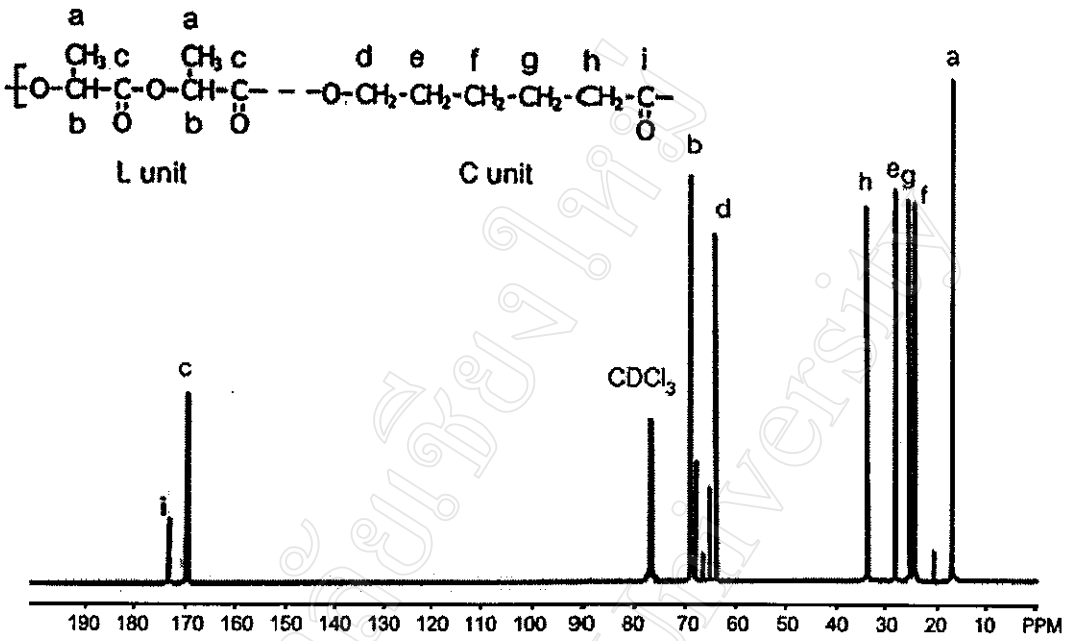

Fig. 4.24 75 MHz ^{13}C-NMR spectrum of the hydroxyl-terminated P(LC) 50 : 50 prepolymer.

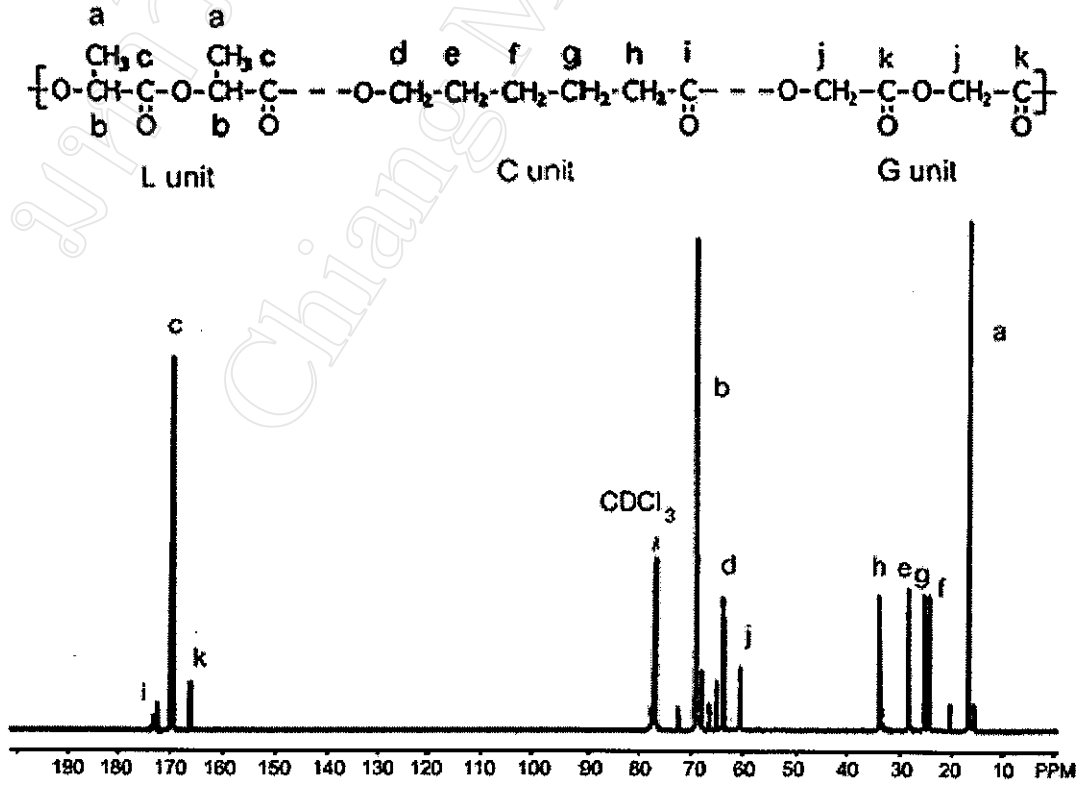

Fig. 4.25 75 MHz ^{13}C-NMR spectrum of the P(LCG) 70 : 20 : 10 triblock terpolymer.

In ^{13}C-NMR polymer spectra, carbonyl (C=O) carbon atoms have been shown to be especially sensitive to sequencing variations, much more so than C-H carbons (methyl, methylene and methine). Therefore, it is the carbonyl region of the spectrum from δ = 165-175 ppm which provides the most information about the co- and terpolymer chain microstructures. When this carbonyl region is expanded, as shown in Figs. 4.26-4.31, various triad sequences, such a CCC, LCC, CCL, LCL, CLL, LLC, LGG, and GGG, can be identified with reference to the homopolymer spectra and related literature reports. Since polyglycolide could not dissolve in $CDCl_3$ as solvent, its carbonyl carbon chemical shift (in hot d_6-DMSO) was also taken from the literature [32].

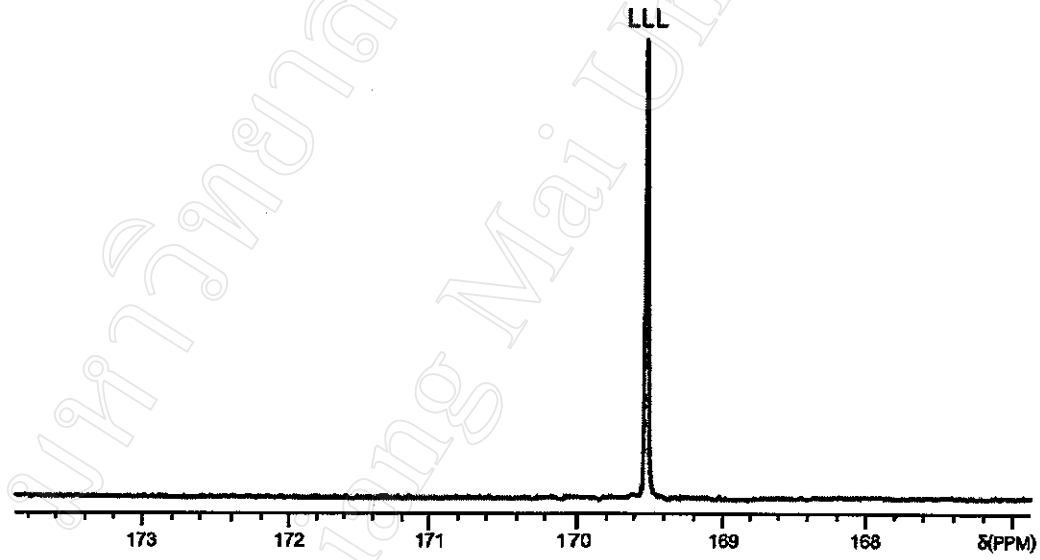

Fig. 4.26 Expanded carbonyl region of the ^{13}C-NMR spectrum of the PL homopolymer.

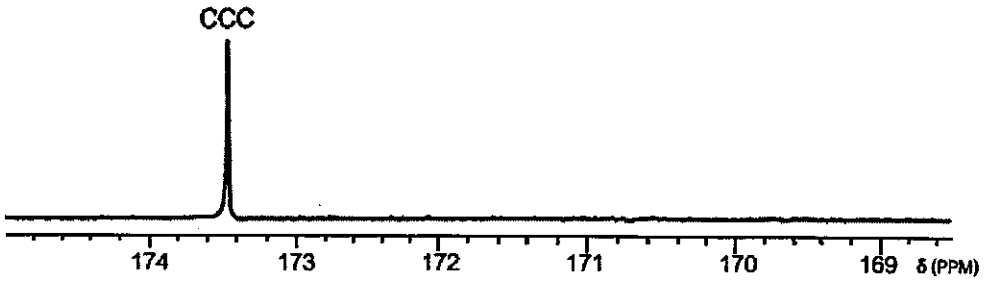

Fig. 4.27 Expanded carbonyl region of the ^{13}C-NMR spectrum of the PCL homopolymer.

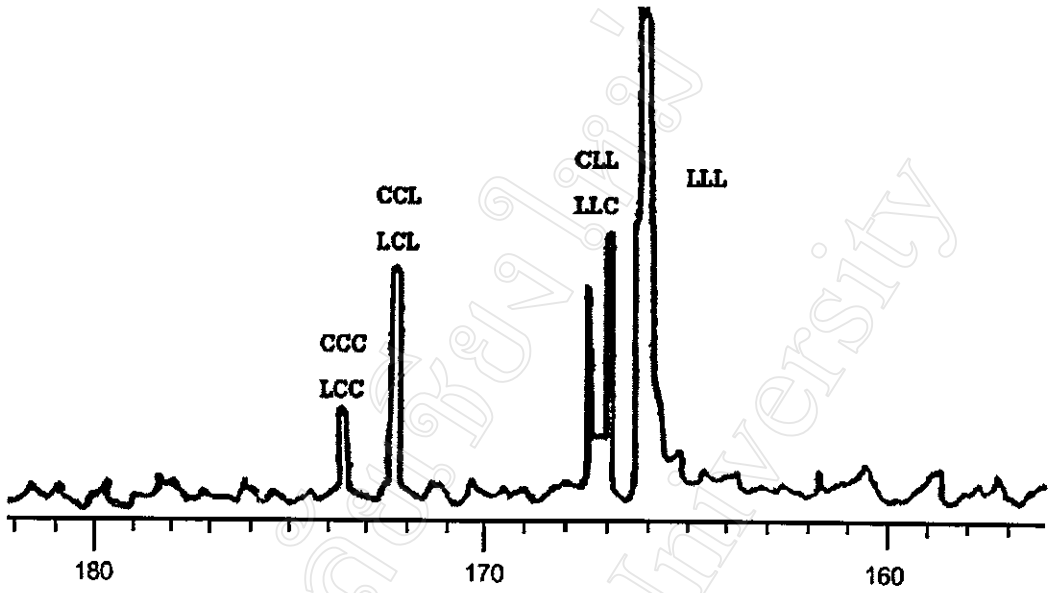

Fig. 4.28 Expanded carbonyl region of the ^{13}C-NMR spectrum of the P(CL) 80 : 20 random copolymer.

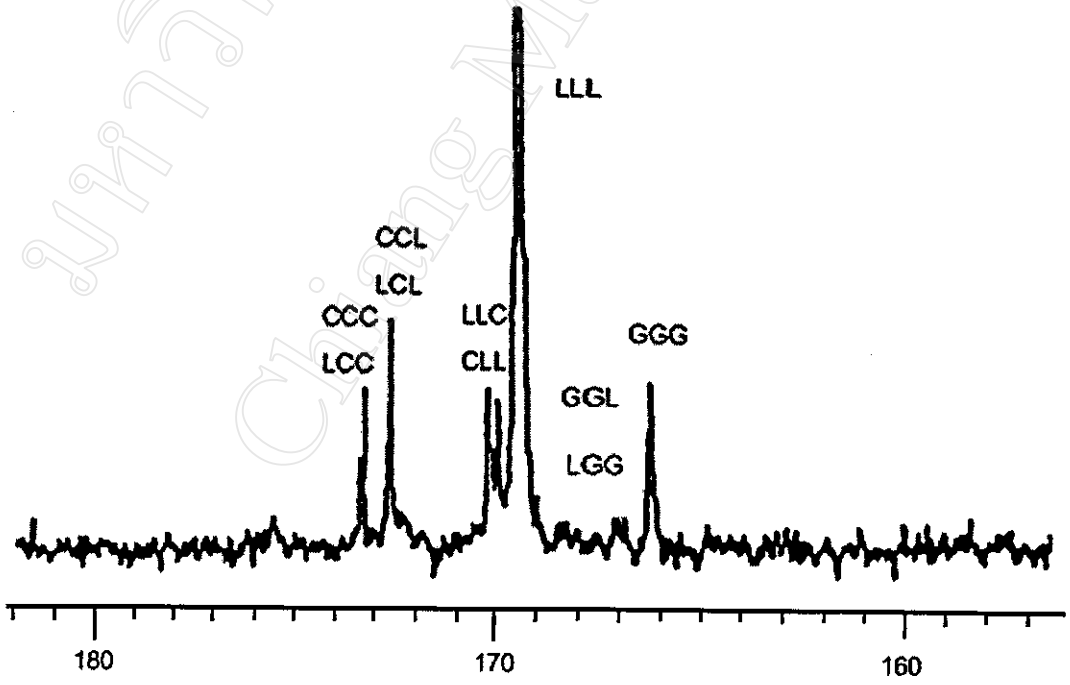

Fig. 4.29 Expanded carbonyl region of the ^{13}C-NMR spectrum of the P(LCG)1 70 : 20 : 10 random terpolymer.

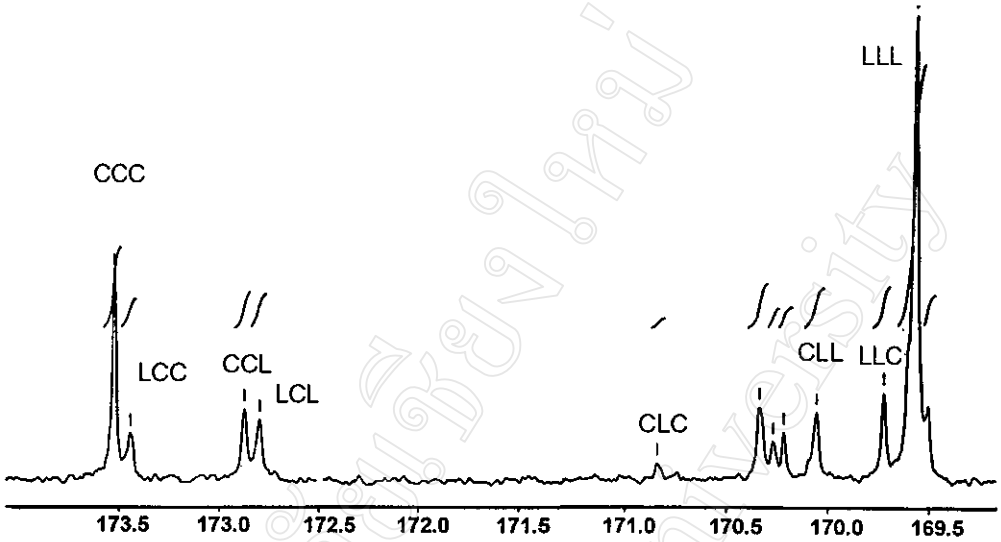

Fig. 4.30 Expanded carbonyl region of the ^{13}C-NMR spectrum of the hydroxyl-terminated P(LC) 50 : 50 prepolymer.

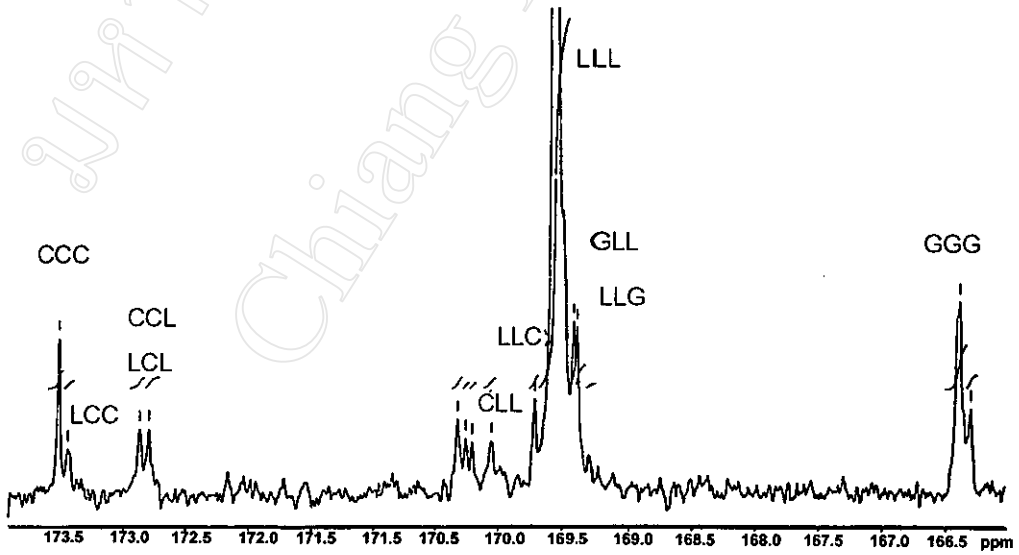

Fig. 4.31 Expanded carbonyl region of the ^{13}C-NMR spectrum of the P(LCG) 70 : 20 : 10 triblock terpolymer.

The expanded spectra of the PL and PCL homopolymers in Figs. 4.26 and 4.27 each show well defined single peaks due to their respective carbonyl carbons at 169.5 ppm (PL) and 173.5 (PCL). When compared with these homopolymer spectra, the P(LC) copolymer spectrum in Fig. 4.28 shows additional small peaks between 169.5 and 173.5 ppm. This indicates the presence of adjoining L and C units which can be identified as those occurring in the various heterounit triad sequences LCC, CCL LCL, LLC and CLL, confirming the random character of the P(LC) copolymer. When the expanded spectrum of the P(LCG) triblock terpolymer in Fig. 4.31 is compared with that of the P(LC) prepolymer in Fig. 4.30, the most striking difference is the marked decrease in the intensities of all peaks between the LLL and CCC peaks while the LLL peak increases due to the preponderance of L units in the end blocks. The peaks between the LLL and GGG (from the G units at 166.4 ppm) peaks also reflect some random character in the L and G units in the end blocks.

The expanded ^{13}C-NMR spectrum of the P(LCG) 1 terpolymer in Fig. 4.29 also shows mixed triad sequences as would be expected in a random terpolymer. The degree of randomness depends upon a variety of factors such as the monomer reactivity ratios, choice of initiator / catalyst, reaction temperature and time, and the extent to which transesterification reactions occur. The control of monomer sequencing is therefore a complex study in itself which, while recognizing its importance, has been beyond the scope of this work.

4.4.3 Thermal Analysis

4.4.3.1 Differential Scanning Calorimetry (DSC)

DSC analyses of the homo-, co- and terpolymer products were conducted at a heating rate of 10°C min^{-1} under dry nitrogen. The DSC thermograms are shown in Figs. 4.32-4.38 and the results compared in Table 4.6.

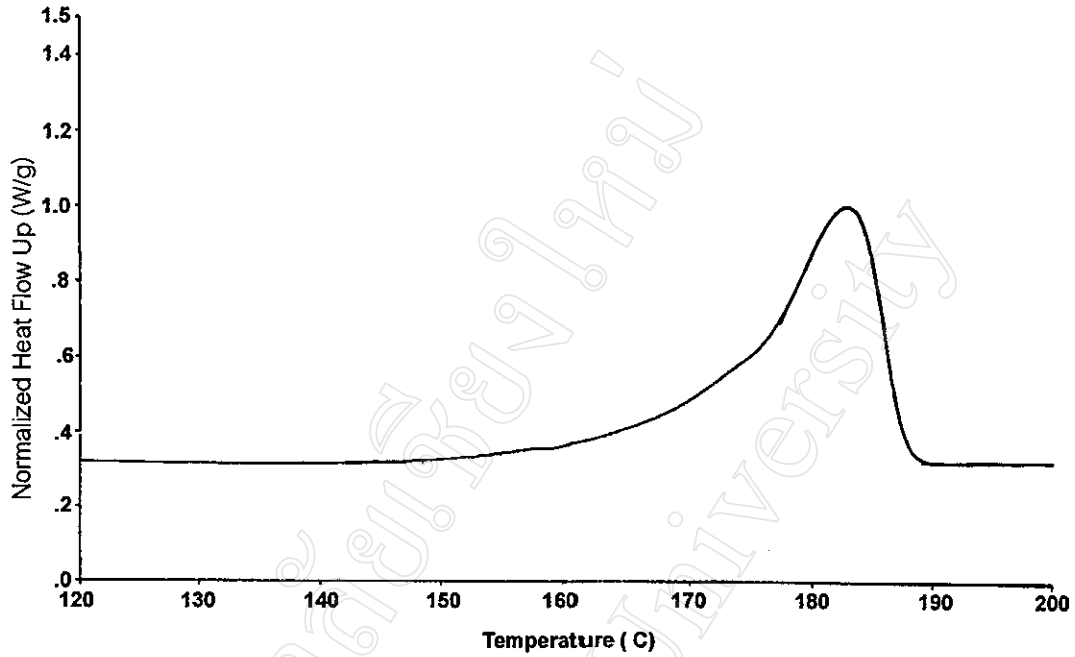

Fig. 4.32 DSC thermogram of the synthesized poly(L-lactide), PL.

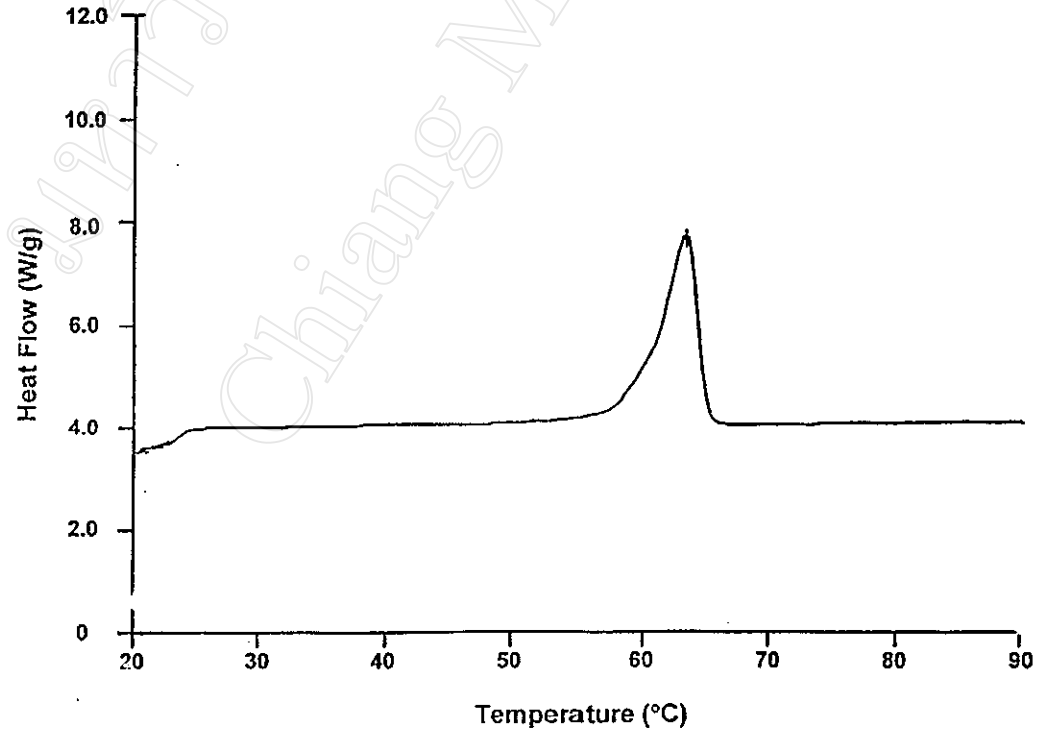

Fig. 4.33 DSC thermogram of commercial poly(ε-caprolactone).

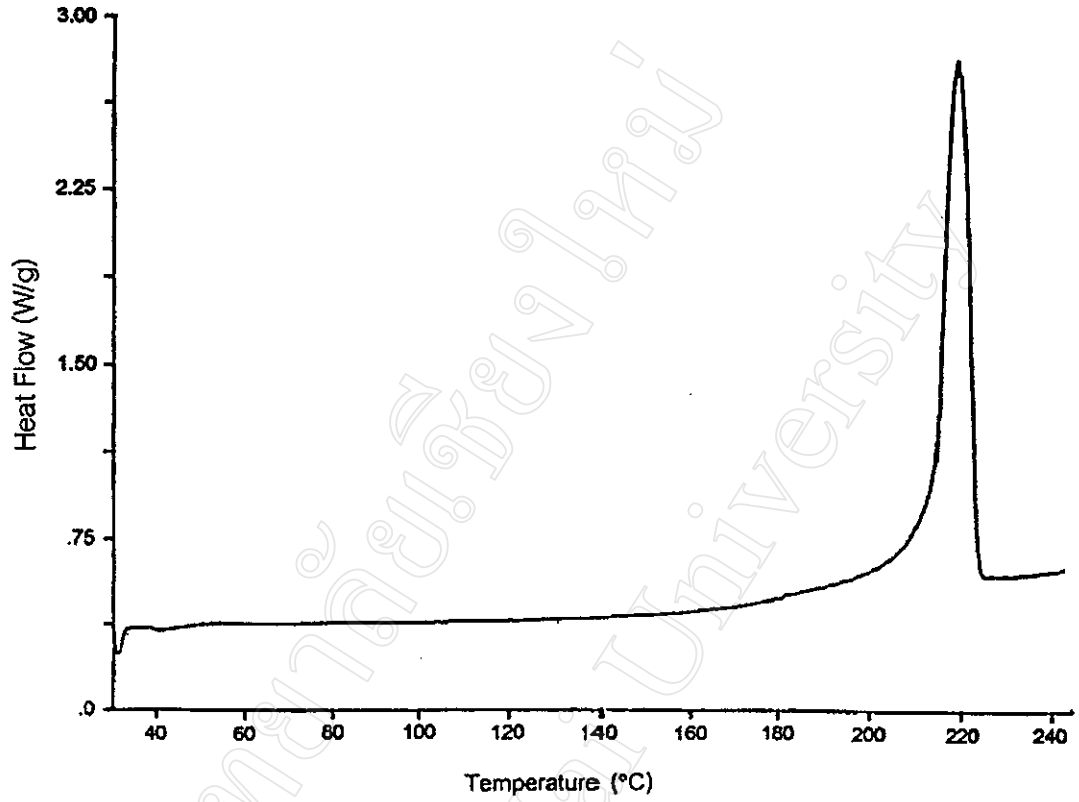

Fig. 4.34 DSC thermogram of polyglycolide [35].

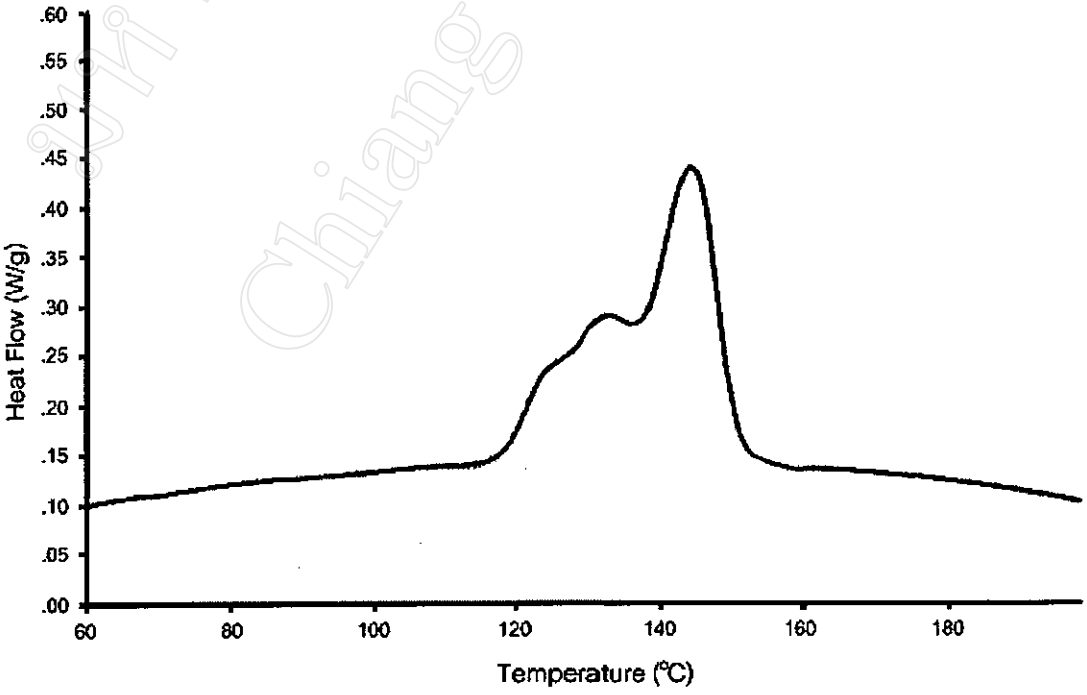

Fig. 4.35 DSC thermogram of the P(LC) 80 : 20 random copolymer.

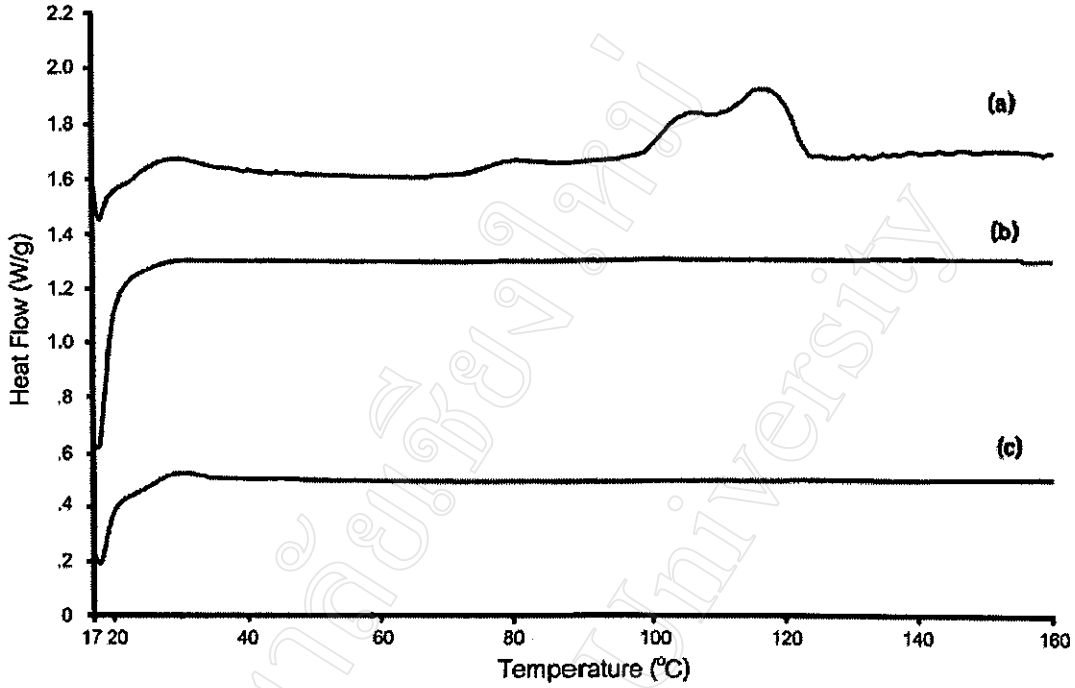

Fig. 4.36 DSC thermograms of the (a) P(LCG)1, (b) P(LCG)2 and (c) P(LCG)3 70 : 20 : 10 random terpolymers.

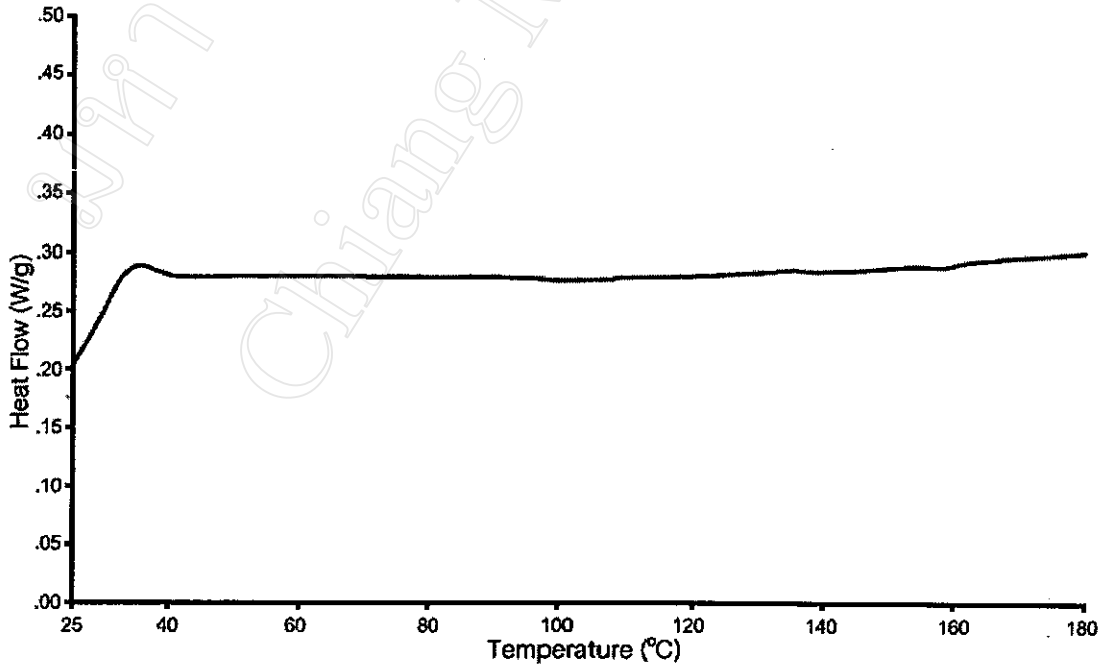

Fig. 4.37 DSC thermogram of the hydroxyl-terminated P(LC) 50 : 50 prepolymer.

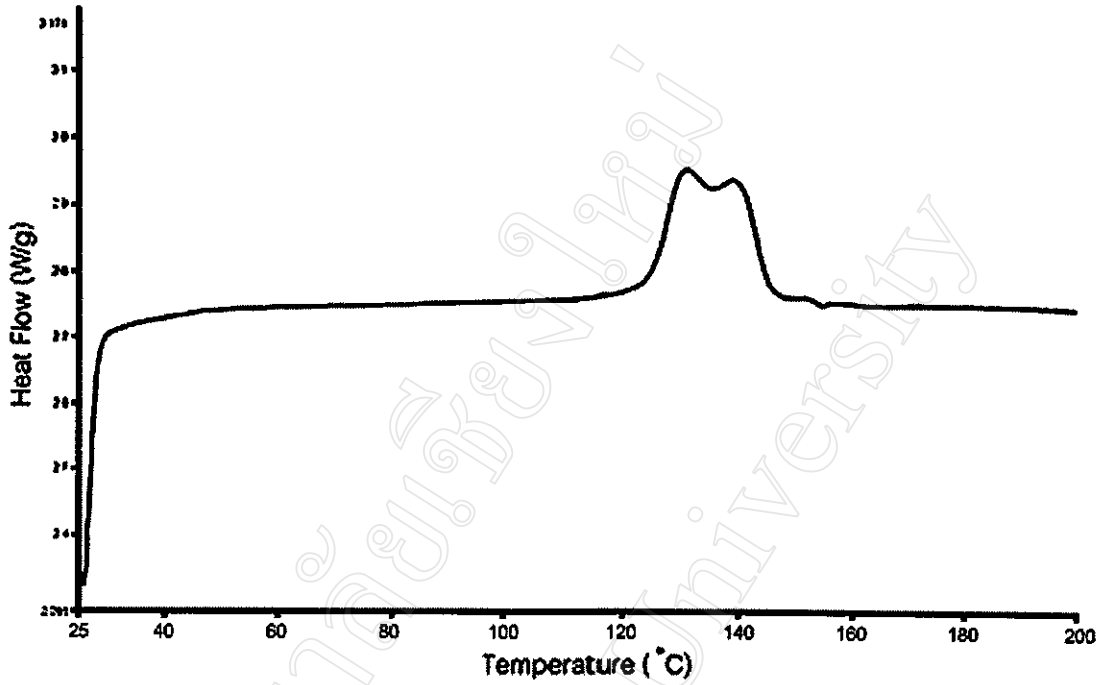

Fig. 4.38 DSC thermogram of the P(LCG) 70 : 20 : 10 triblock terpolymer.

From the previous DSC thermograms, the 3 homopolymers each show well-defined melting transitions, T_m, (Figs. 4.32-4.34) which reflect their semi-crystalline morphology. However, as other monomer units are introduced into the poly(L-lactide) chain, this semi-crystalline morphology becomes disrupted due to the increased structural irregularity. For example, the melting peak of the P(LC) 80 : 20 random copolymer (Fig. 4.35) is both broader, smaller in area, and shifted to a lower temperature range than that in PL due to the random incorporation of the C units. This is also true of the P(LCG) 1 random terpolymer in Fig. 4.36(a). Interestingly, the other two random terpolymers, P(LCG)2 and P(LCG)3, show no melting peak at all (Fig. 4.36(b) and (c)), indicating that they are completely amorphous. This demonstrates how the different conditions used in synthesis (in this case, different initiator / catalyst ratios) can also affect the monomer sequence distribution and, hence, the morphology of the final product. Similarly, the P(LC) 50 : 50 random prepolymer (Fig. 4.37) is also completely amorphous as would be expected but, when the LG end-blocks are added on, the P (LCG) triblock becomes semi-crystalline.

In all of the co- and terpolymers synthesized here, the glass transition temperatures, T_g, could not be determined with certainly since they were either below or in the region of ambient temperature. The DSC instrument used in this work could only operate at ambient temperature and above. Furthermore, determination of the T_g in co- and terpolymers is made even more difficult by the compositional drift along the chain. This effect tends to broaden the T_g and, in doing so, often renders it difficult to distinguish against the background of the baseline drift.

Table 4.6 DSC transition temperatures and heats of melting of the homo-, co-, and terpolymers.

Polymer	T_g (°C)	T_m [a] (°C)	ΔH_m [b] (J g^{-1})
Homopolymers			
Poly(L-lactide)	60(65)[c]	183	50.3
Poly(ε-caprolactone)	nd (-60)[c]	60	89.8
Polyglycolide	nd (35)[c]	217	102.8
P(LCG) random terpolymers (70 : 20 : 10)			
P(LCG)1	nd	109	11.2
P(LCG)2	nd	nd	nd
P(LCG)3	nd	nd	nd
P(LC) copolymer (80 : 20)	nd	144	30.2
P(LC) prepolymer (50 : 50)	nd	nd	nd
P(LCG) triblock terpolymer	nd	131	18.6

[a] T_m taken as the peak temperature of the melting range

[b] $\Delta H_m \propto$ area under the melting peak $\propto$ % crystallinity

[c] reference T_g values in parentheses obtained from reference [1]

nd = not detected or difficult to estimate accurately

4.4.3.2 Thermogravimetry (TG)

The dynamic (non-isothermal) TG thermograms in Figs. 4.39-4.44 compare and contrast the thermal degradation profiles of all of the polymers studied. In each case, a heating rate of 20°C min^{-1} was used under an inert flowing nitrogen atmosphere. The temperature ranges over which the weight losses occurred are compared in Table 4.7.

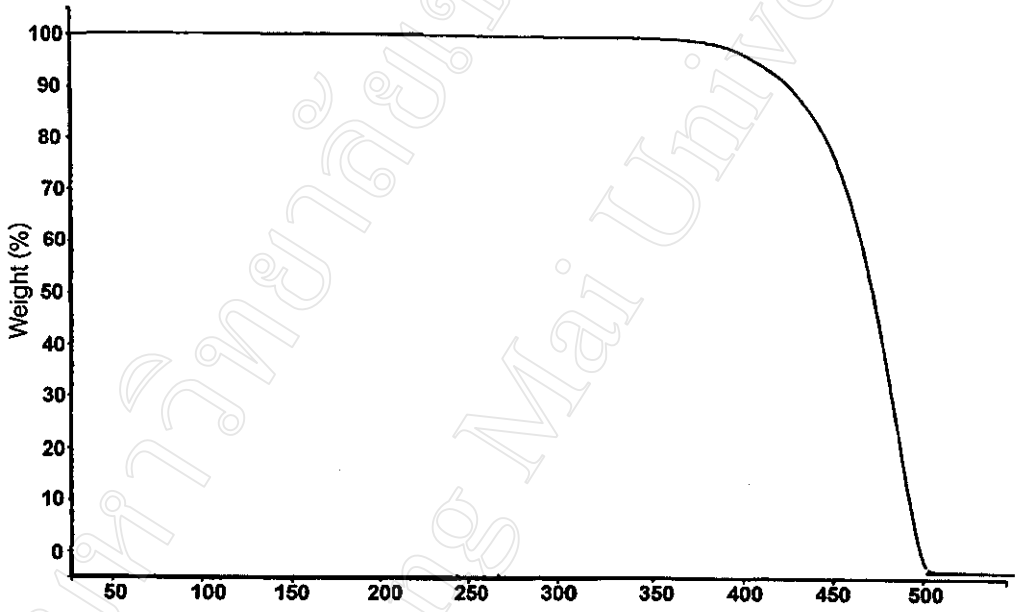

Fig. 4.39 TG thermogram of the synthesized poly(L-lactide), PL.

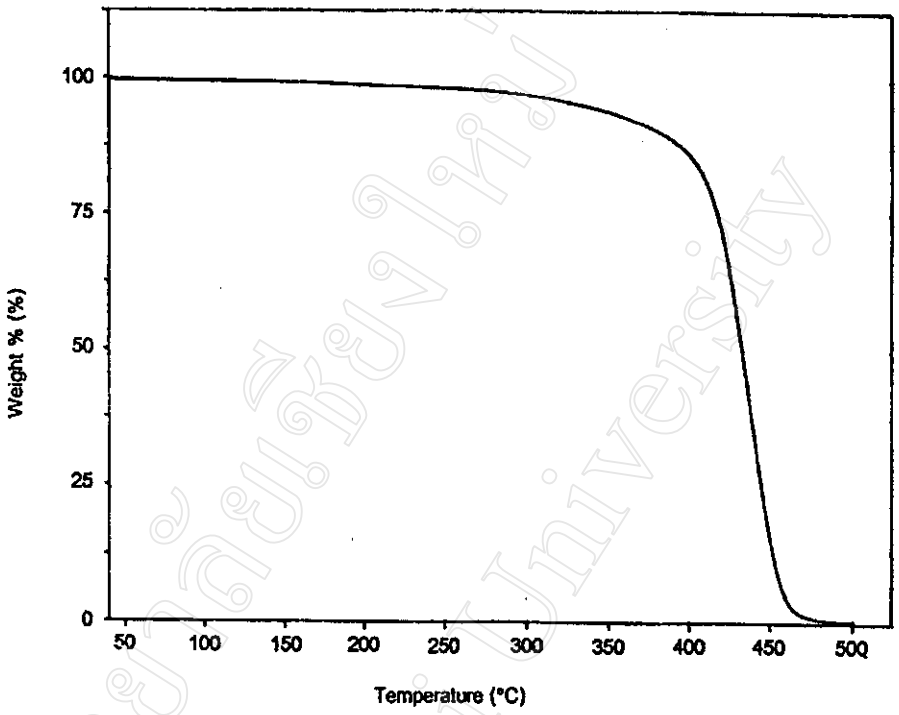

Fig. 4.40 TG thermogram of commercial poly(ε-caprolactone).

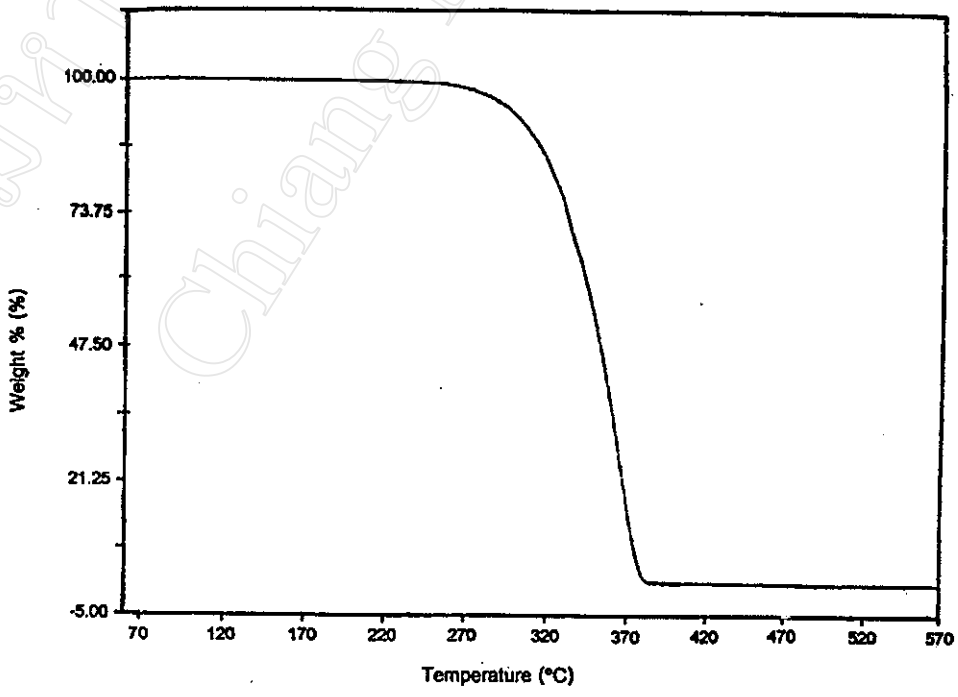

Fig. 4.41 TG thermogram of polyglycolide [62].

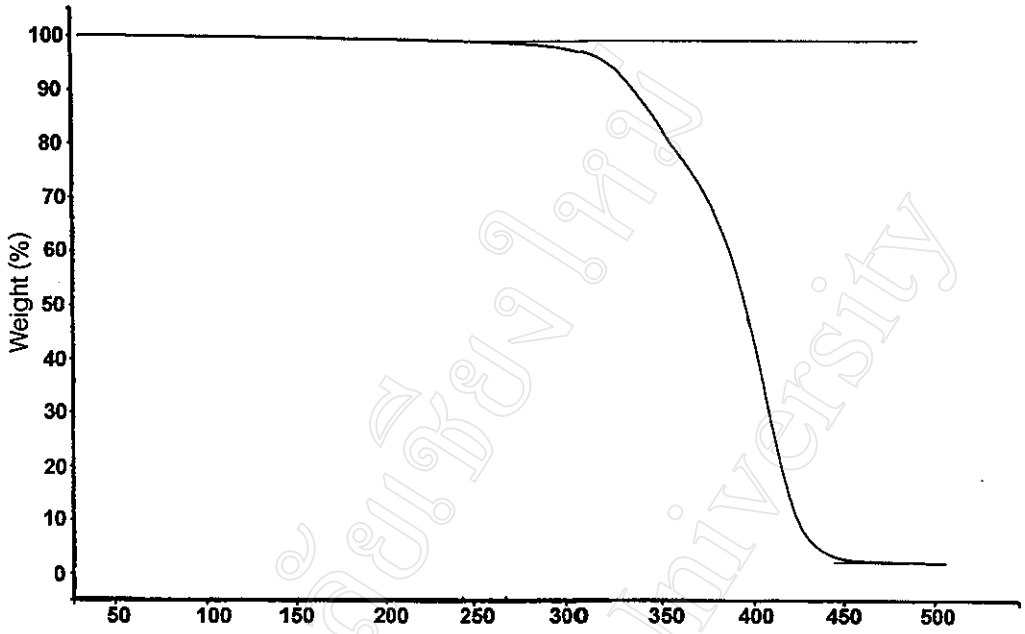

Fig. 4.42 TG thermogram of the P(LC) 80 : 20 random copolymer.

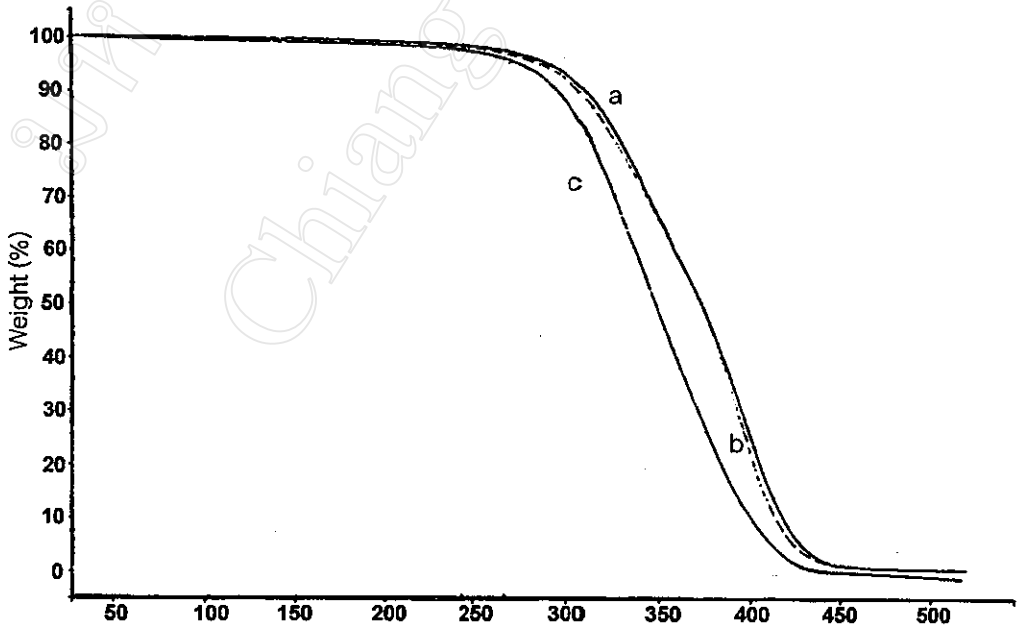

Fig. 4.43 TG thermograms of the P(LCG) 70 : 20 : 10 random terpolymers.
(a) P(LCG)1 (b) P(LCG)2 (c) P(LCG)3

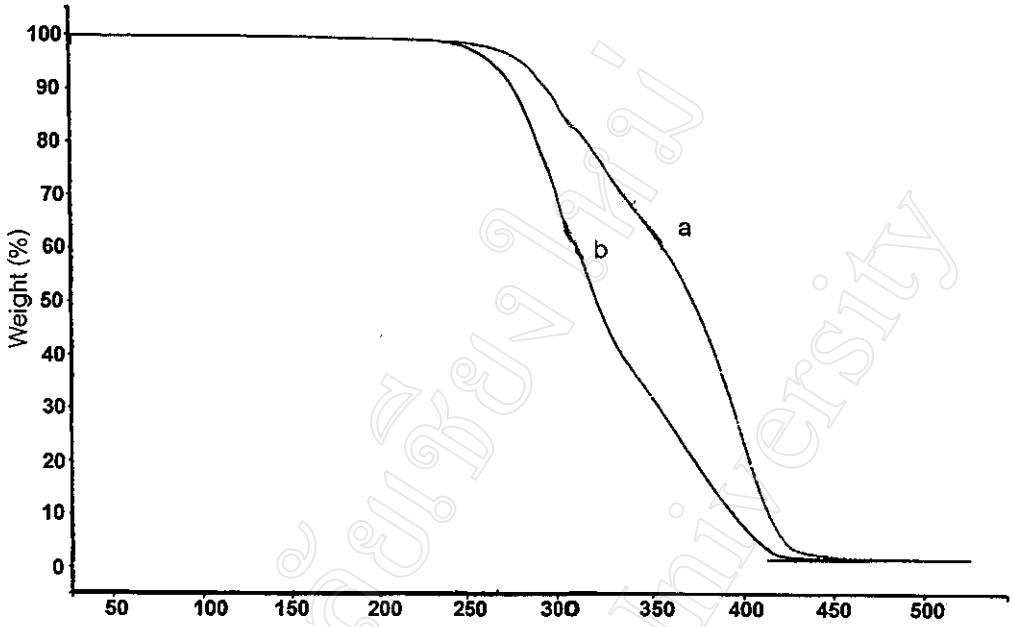

Fig. 4.44 TG thermograms of (a) the P(LC) 50 : 50 prepolymer and (b) the P(LCG) 70 : 20 : 10 triblock terpolymer.

The main purpose of this TG study was to define the upper temperature limits for fibre processing below which the homo-, co-, and terpolymers could be safely melt spun without accompanying degradation. Thus, the DSC and TG data together defined the melt processing range. As a rough guide, this melt processing range is usually considered to be approximately:

$$T_m + 10^{\circ}C \longrightarrow T_d - 50^{\circ}C$$

lower limit upper limit

where T_m = melting point

and T_d = initial weight loss temperature

However, as explained in the previous Chapter 3, and especially where aliphatic polyesters are concerned, the actual processing range is often much narrower than this approximation suggests. In practice, it is always better to gravitate towards the lower end of this range as much as the melt viscosity and filament line stability will allow.

Table. 4.7 TG thermal degradation ranges for the polymer products studied.

Polymer	Thermal Degradation Range (°C)
Homopolymers	
Poly(L-lactide)	200 – 400
Poly(ε-caprolactone)	210 – 470
Polyglycolide	230 – 410
P(LCG) random terpolymer (70 : 20 : 10)	
P(LCG)1	200 – 470
P(LCG)2	180 – 450
P(LCG)3	220 – 470
P(LC) copolymer (80 : 20)	220 – 450
P(LC) prepolymer (50 : 50)	250 – 480
P(LCG) triblock terpolymer	250 – 460

4.4.4 Molecular Weight Determination

4.4.4.1 Dilute-Solution Viscometry

The intrinsic viscosities, [η], of the polymer products were measured with a Ubbelohde viscometer in $CHCl_3$ as solvent at 30°C. The results are summarized in Table 4.8. With the exception of the poly(L-lactide) homopolymer, these (η) values could not be converted into average molecular weights because the constants 'K' and 'a' in the Mark – Houwink – Sakurada Equation ($[\eta] = K\bar{M}_v^a$) are unknown for the co- and terpolymers. However, for poly(L-lactide) homopolymer in chloroform at 30°C, the following equation is available in the literature [63]

$$[\eta] = 1.29 \times 10^{-4} \overline{M}_v^{0.82} \quad dl\ g^{-1}$$

from which the value of $[\eta]$ = 0.96 dl g^{-1} in Table 4.8 yields a value for the viscosity-average molecular weight, $\overline{M}_v$, of

$$\overline{M}_v = 5.00 \times 10^4$$

which is generally considered to be in the medium molecular weight range for PL.

As for the co- and terpolymers, their $[\eta]$ values in Table 4.8 suggest molecular weights of a similar order, as confirmed by their GPC data.

4.4.4.2 Gel Permeation Chromatography (GPC)

The average molecular weights and polydispersity indices of the polymers were determined by gel permeation chromatography (GPC). The GPC measurements were performed in $CHCl_3$ as eluent with a flow-rate of 1 ml min^{-1} using a Waters 150 CV Gel Permeation Chromatograph. This instrument was equipped with an Ultrastyragel® column operating at 30°C and employing both differential refractometry and on-line viscometry detectors with universal calibration. Examples of some of the GPC curves obtained are shown in Figs. 4.41-4.44 while the various molecular weight averages and polydispersity indices are compared in Table 4.8.

It is notable that all of the GPC curves show unimodal molecular weight distributions despite the compositional heterogeneities of the co- and terpolymers. This is particularly significant in the case of the P(LCG) triblock copolymer since it provides supporting evidence that the copolymerisation of L-lactide and glycolide in the second step of the synthesis did indeed occur at the two chain ends of the P(LC) prepolymer. Had this not been the case, a polymer blend would have been formed which would probably have shown a bimodal distribution instead.

As far as the actual values are concerned, $\bar{M}_n$ values in excess of 40,000 are generally considered to be adequate for melt spinning which was the main objective of the synthesis work. Higher molecular weights ($\bar{M}_n$ > 100,000) would have been better still but would have required a much more detailed study of the synthesis conditions.

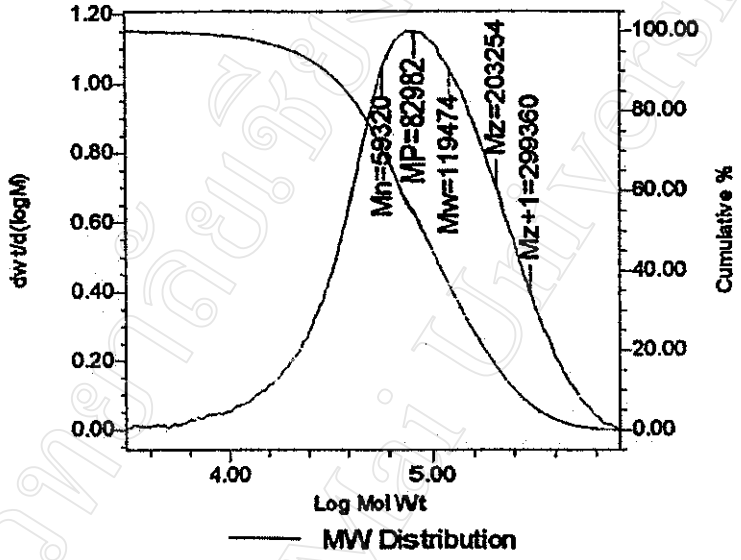

Fig. 4.45 GPC curve of the P(LC) 80 : 20 random copolymer.

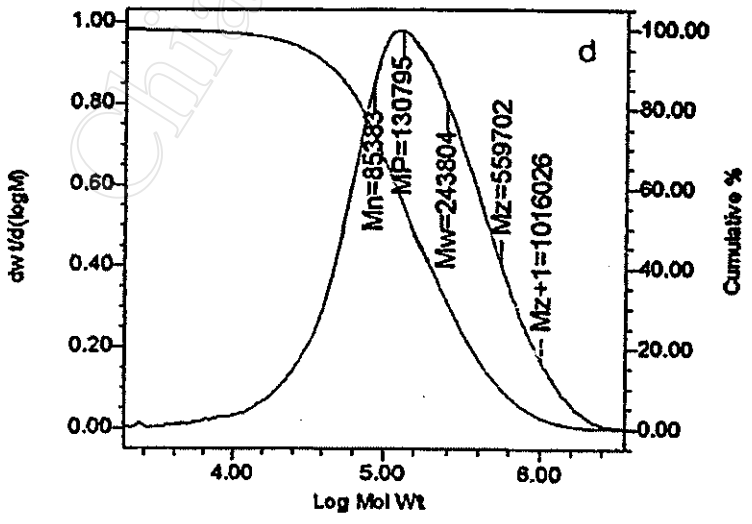

Fig. 4.46 GPC curve of the P(LCG)1 70 : 20 : 10 random terpolymer.

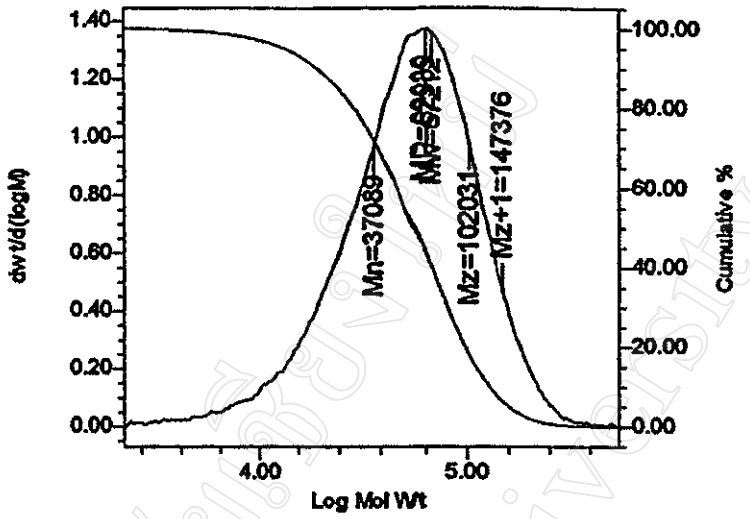

Fig. 4.47 GPC curve of the P(LC) 50 : 50 prepolymer.

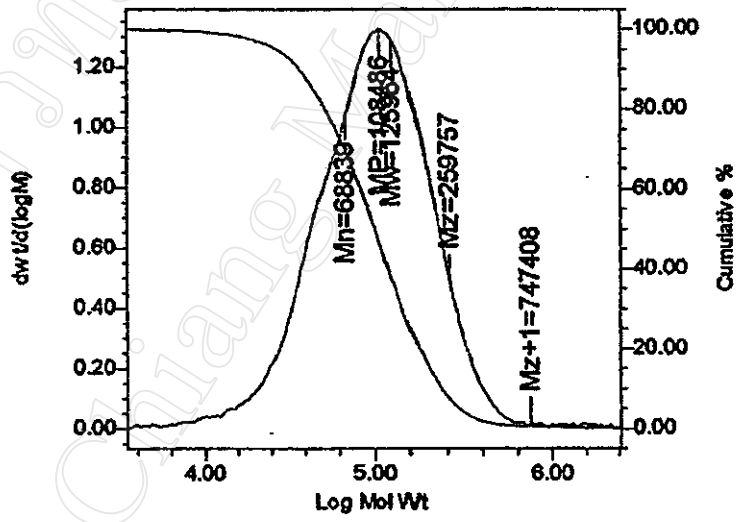

Fig. 4.48 GPC curve of the P(LCG) 70 : 20 : 10 triblock terpolymer.

Table 4.8 Molecular weight data relating to the polymer products.

Polymer	$[\eta]^a$	Average Molecular Weights [b]			
	(dl g^{-1})	$\bar{M}_v$	$\bar{M}_n$	$\bar{M}_w$	$\bar{M}_w/\bar{M}_n$ [c]
Homopolymer					
Poly(L-lactide)	0.96	50,007	-	-	-
Random terpolymers (70 : 20 : 10)					
P(LCG)1	1.38	-	85,383	243,804	2.86
P(LCG)2	1.03	-	43,335	91,565	2.38
P(LCG)3	1.18	-	-	-	-
P(LC) copolymer (80 : 20)	1.44	-	59,350	119,474	2.01
P(LC) prepolymer (50 : 50)	0.81	-	37,089	67,212	1.81
P(LCG) triblock	1.15	-	68,839	125,964	1.83

[a] as determined in $CHCl_3$ as solvent at 30°C

[b] values as read from the GPC data print-outs without adjustment for significant figures

[c] $\bar{M}_w/\bar{M}_n$ = polydispersity ratio